Synthesis, Structural Studies, and Photophysical Properties of Heteroleptic Inverse-Coordination Clusters

Guan-Rong Huang,[a] Rhone P. Brocha Silalahi,[a] Jian-Hong Liao,[a] Tzu-Hao Chiu,[a] and C. W. Liu[a]*

[a] Department of Chemistry, National Dong Hwa University No. 1, Sec. 2, Da Hsueh Rd. Shoufeng, Hualien, Taiwan 974301 (R.O.C.) E-mail:chenwei@gms.ndhu.edu.tw

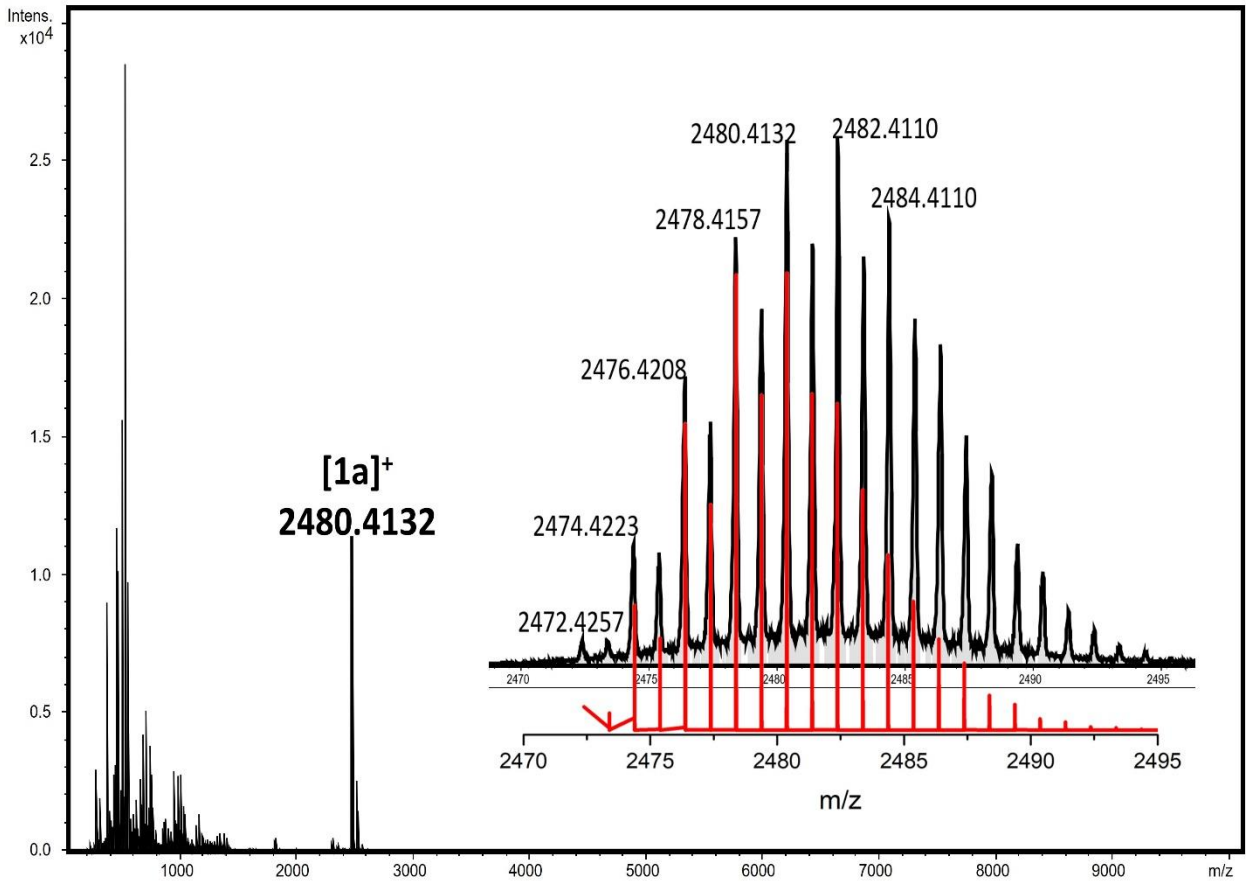

Figure S1. ESI-MS spectra of the cluster [**1a**-PF_6]$^+$ in positive mode. Inset: Experimental in the top (black) and theoretical one in the bottom (red) of [**1a**-PF_6]$^+$.

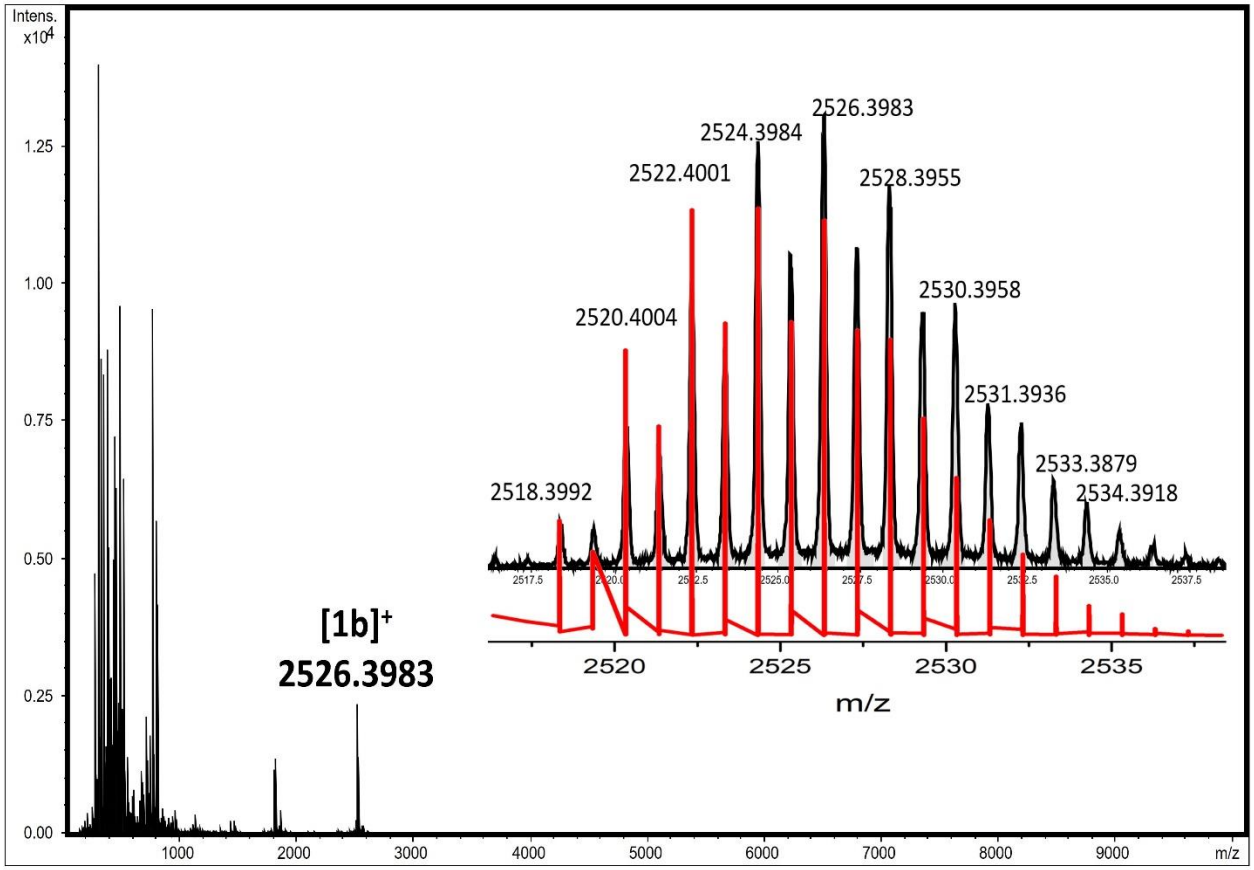

Figure S2. ESI-MS spectra of the cluster [**1b**-PF_6]$^+$ in positive mode. Inset: Experimental in the top (black) and theoretical one in the bottom (red) of [**1b**-PF_6]$^+$.

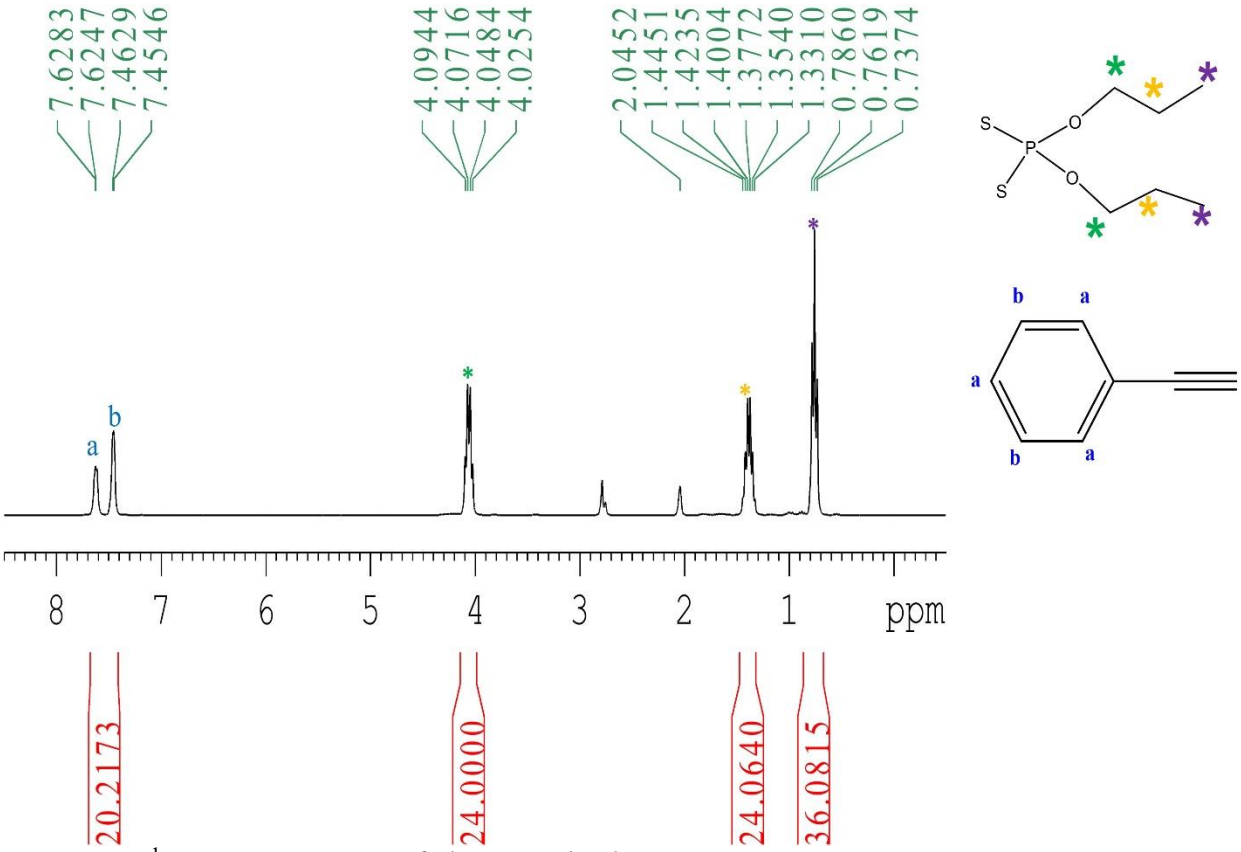

Figure S3. ^{1}H NMR spectrum of cluster **1a** in d_6-acetone.

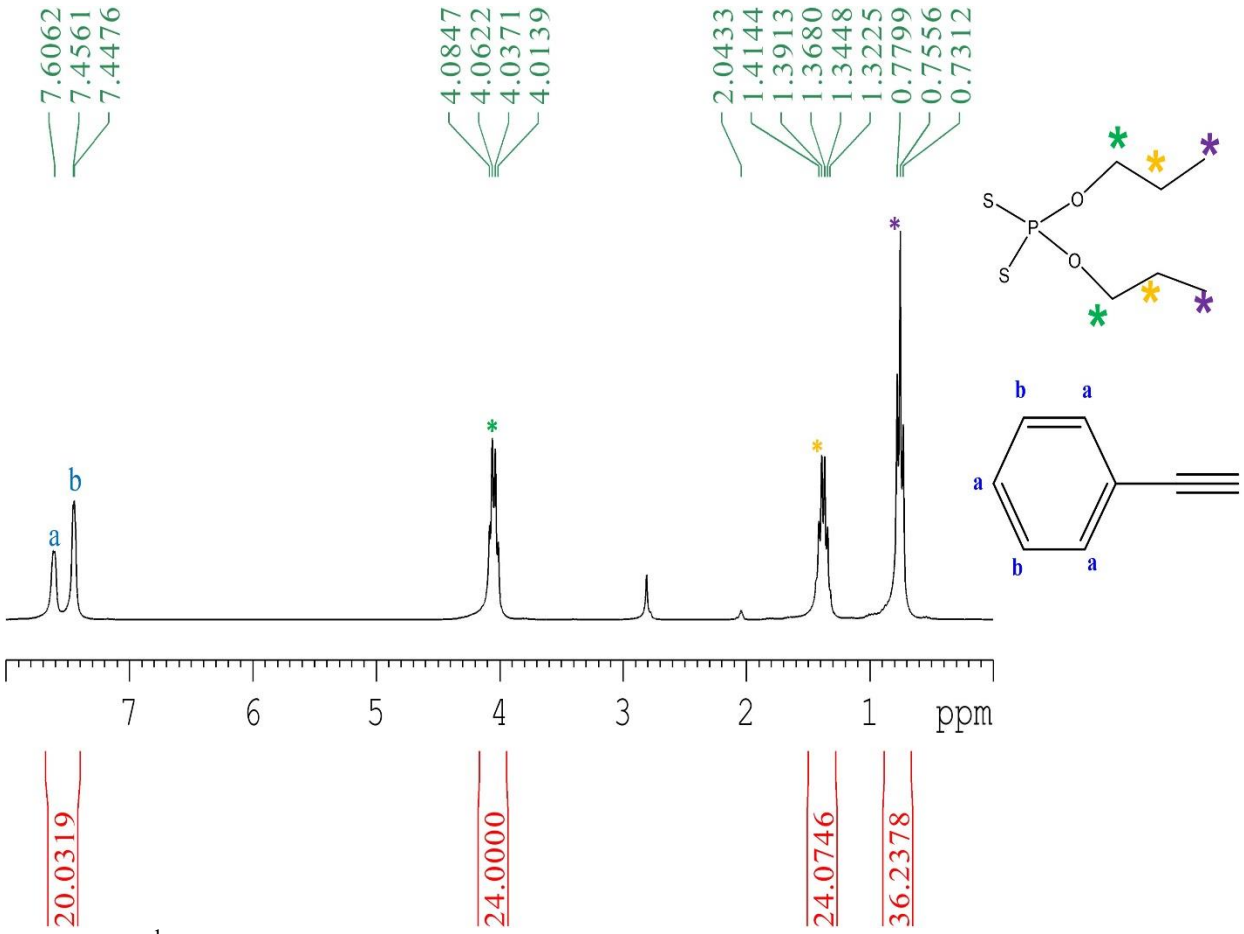

Figure S4. ^{1}H NMR spectrum of cluster **1b** in d_6-acetone.

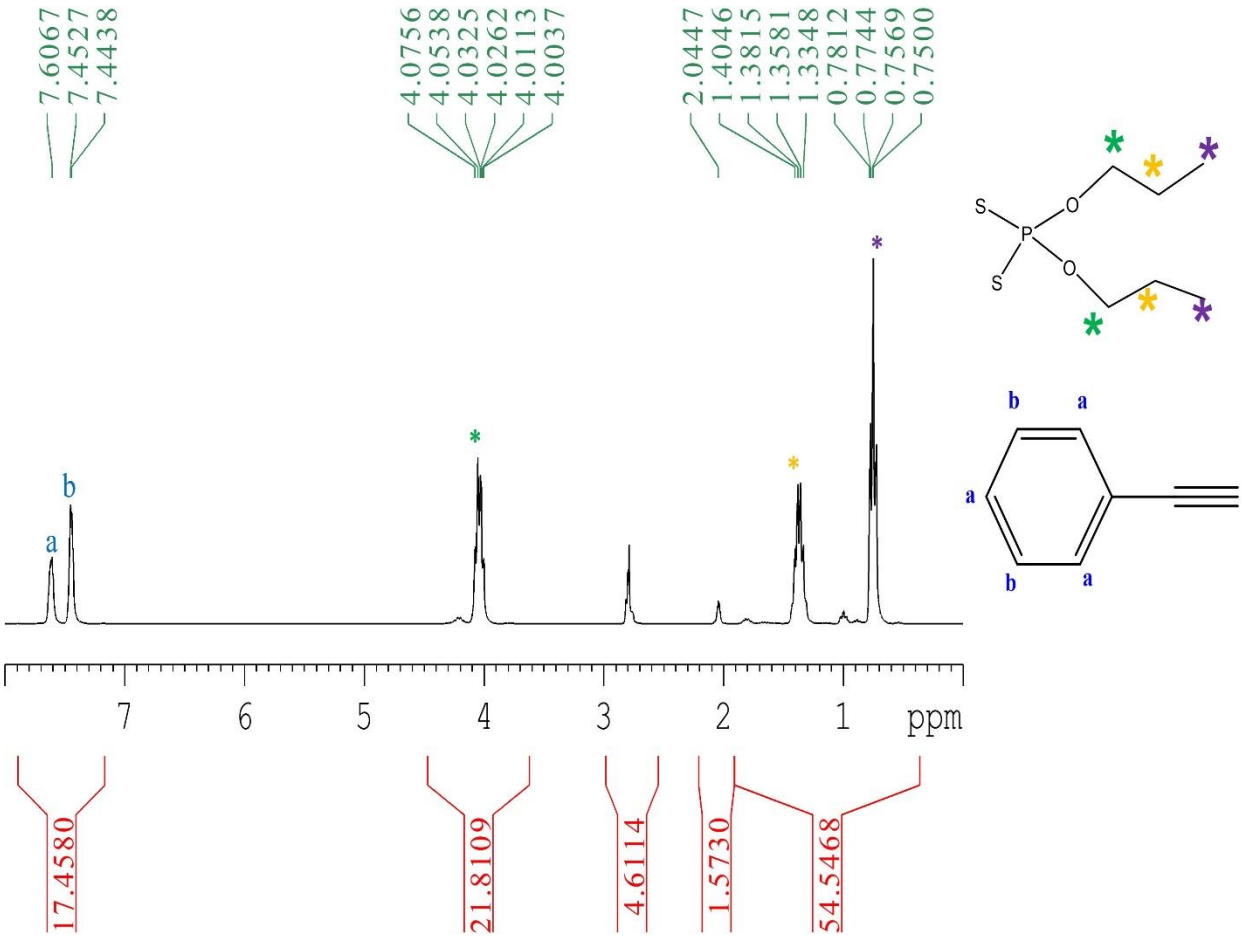

Figure S5. ^{1}H NMR spectrum of cluster **1c** in d_6-acetone.

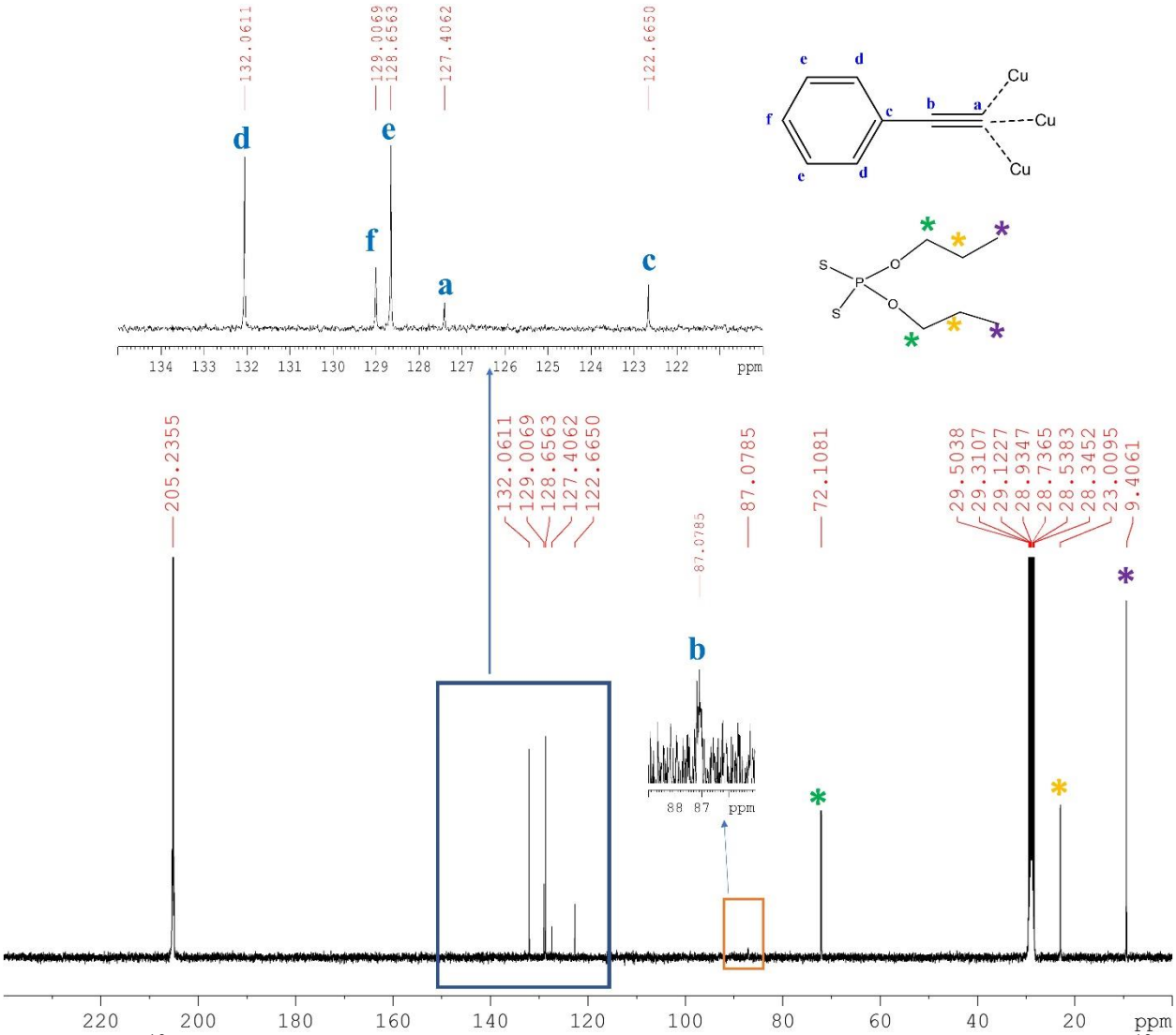

Figure S6. ^{13}C NMR spectrum of cluster **1a** in d_6-acetone. Inset; the expanded spectra for ^{13}C NMR of phenyl rings. The (*, *, and *) highlighted are the ^{13}C NMR of the ^{i}Pr alkyl group in the dithiophosphate ligand.

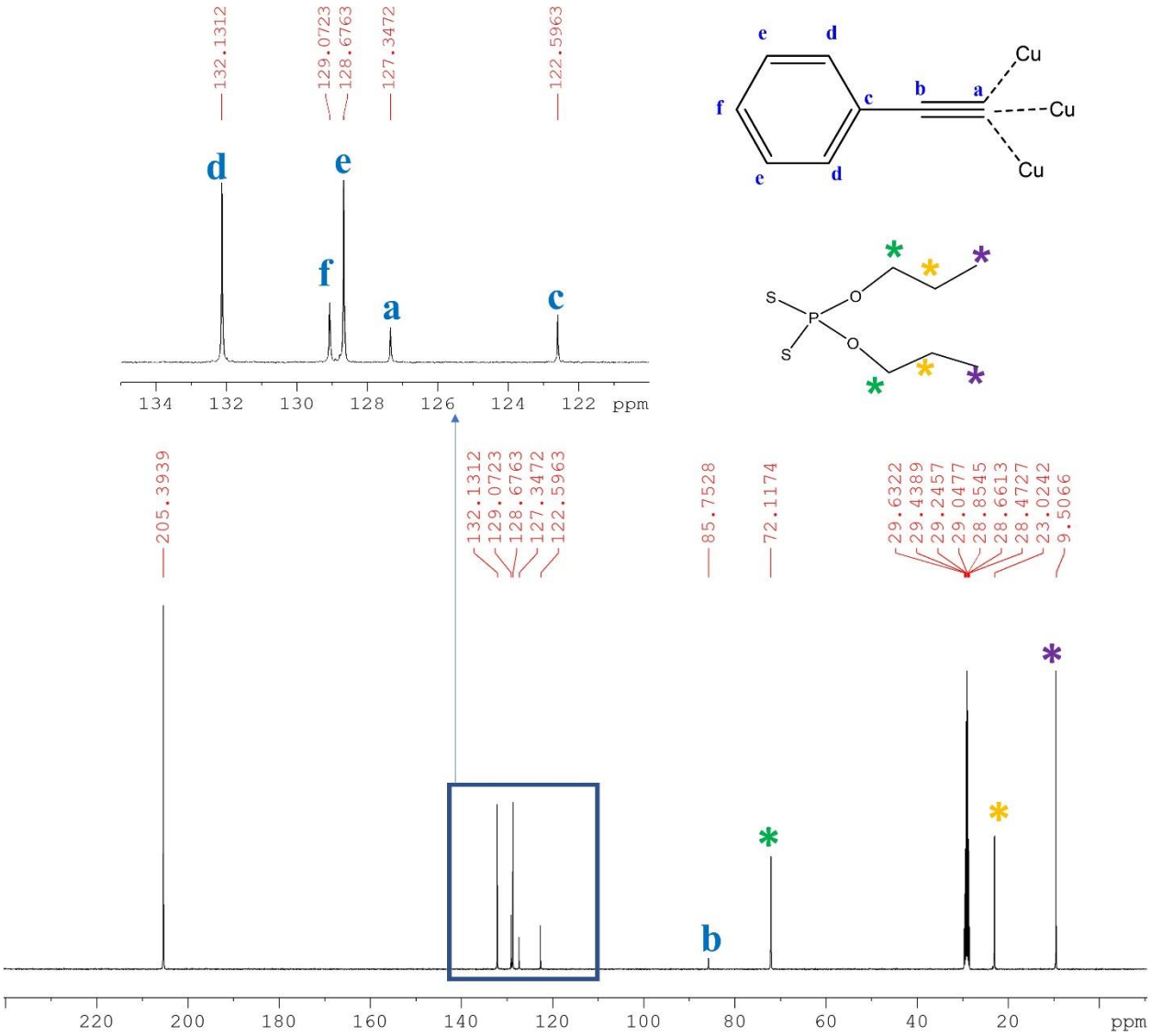

Figure S7. ^{13}C NMR spectrum of cluster **1b** in d_6-acetone. Inset; the expanded spectra for ^{13}C NMR of phenyl rings. The (*, *, and *) highlighted are the ^{13}C NMR of the ^{i}Pr alkyl group in the dithiophosphate ligand.

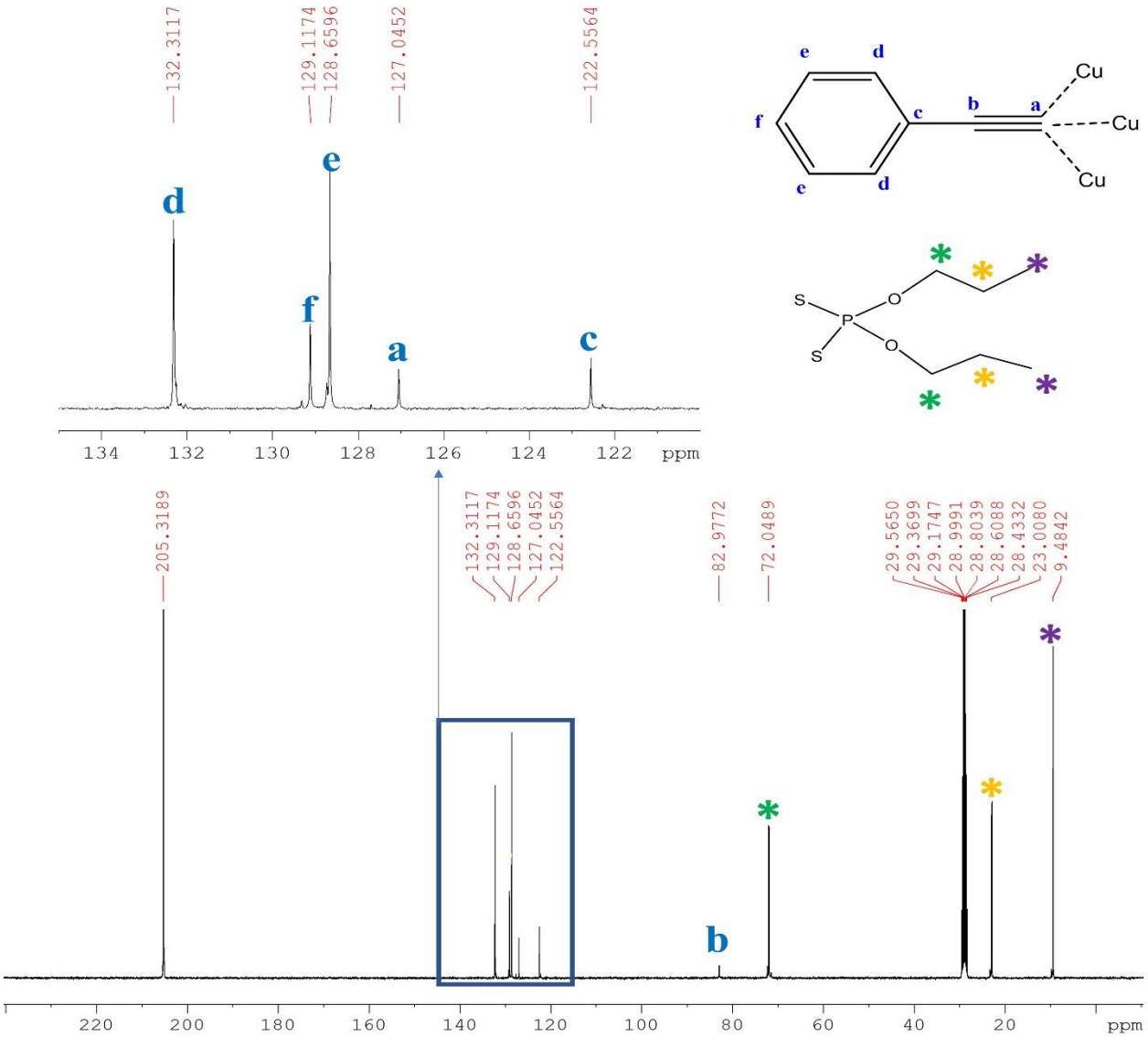

Figure S8. ^{13}C NMR spectrum of cluster **1c** in *d*$_6$-acetone. Inset; the expanded spectra for ^{13}C NMR of phenyl rings. The (*, *, and *) highlighted are the ^{13}C NMR of the ^{i}Pr alkyl group in the dithiophosphate ligand.

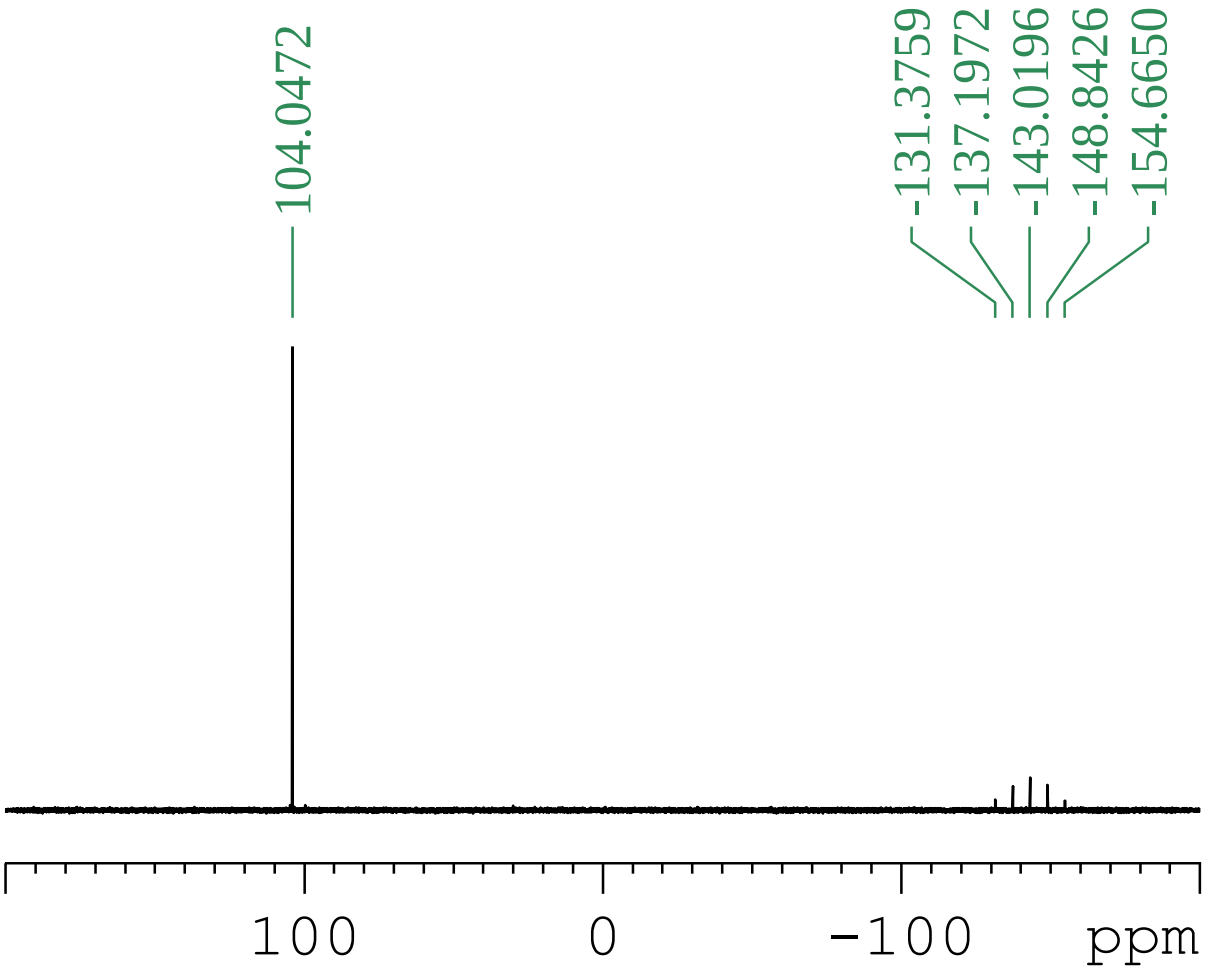

Figure S9. $^{31}P\{^{1}H\}$ NMR spectrum of cluster **1a** in d_6-acetone.

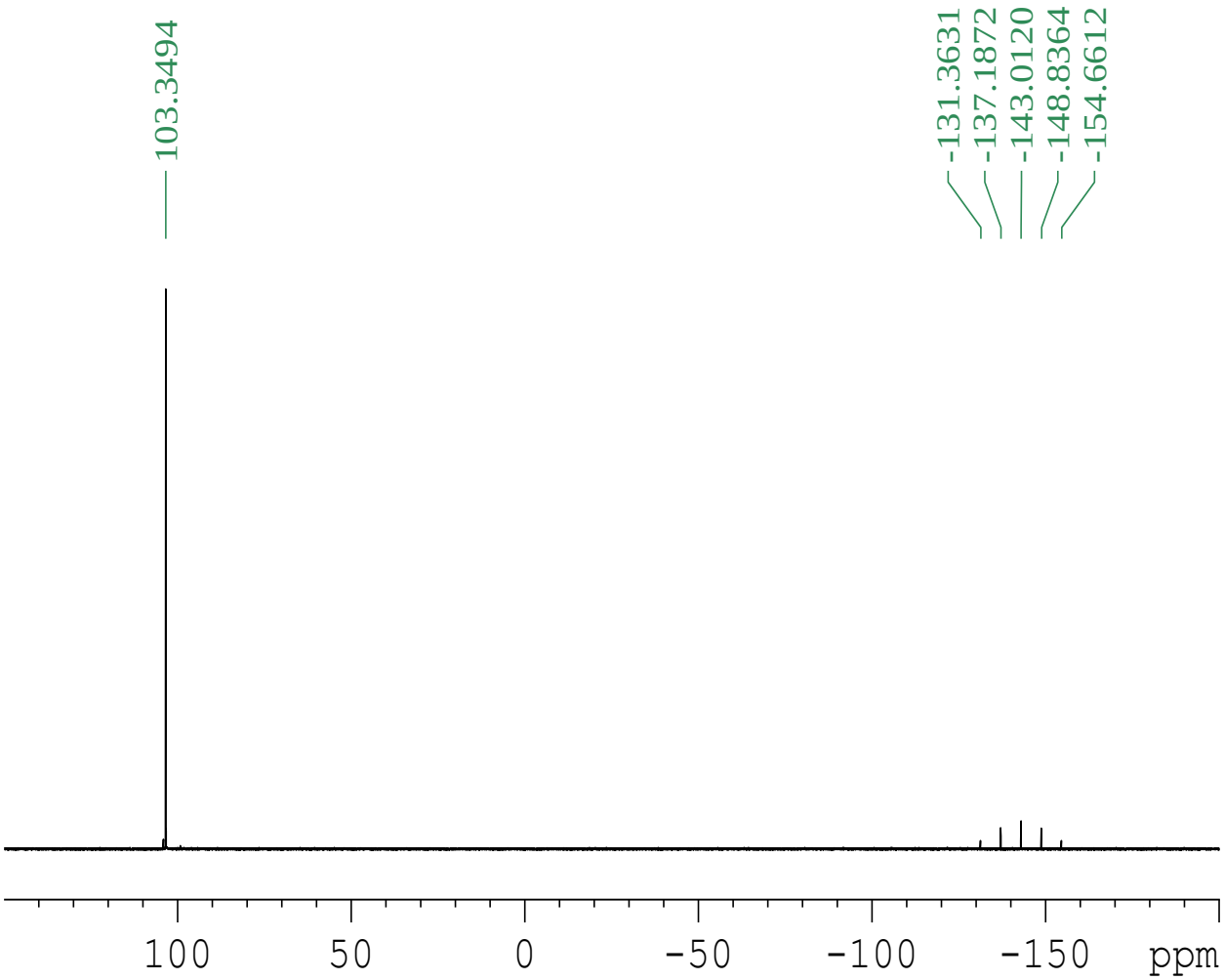

Figure S10. $^{31}P\{^{1}H\}$ NMR spectrum of cluster **1b** in d_6-acetone.

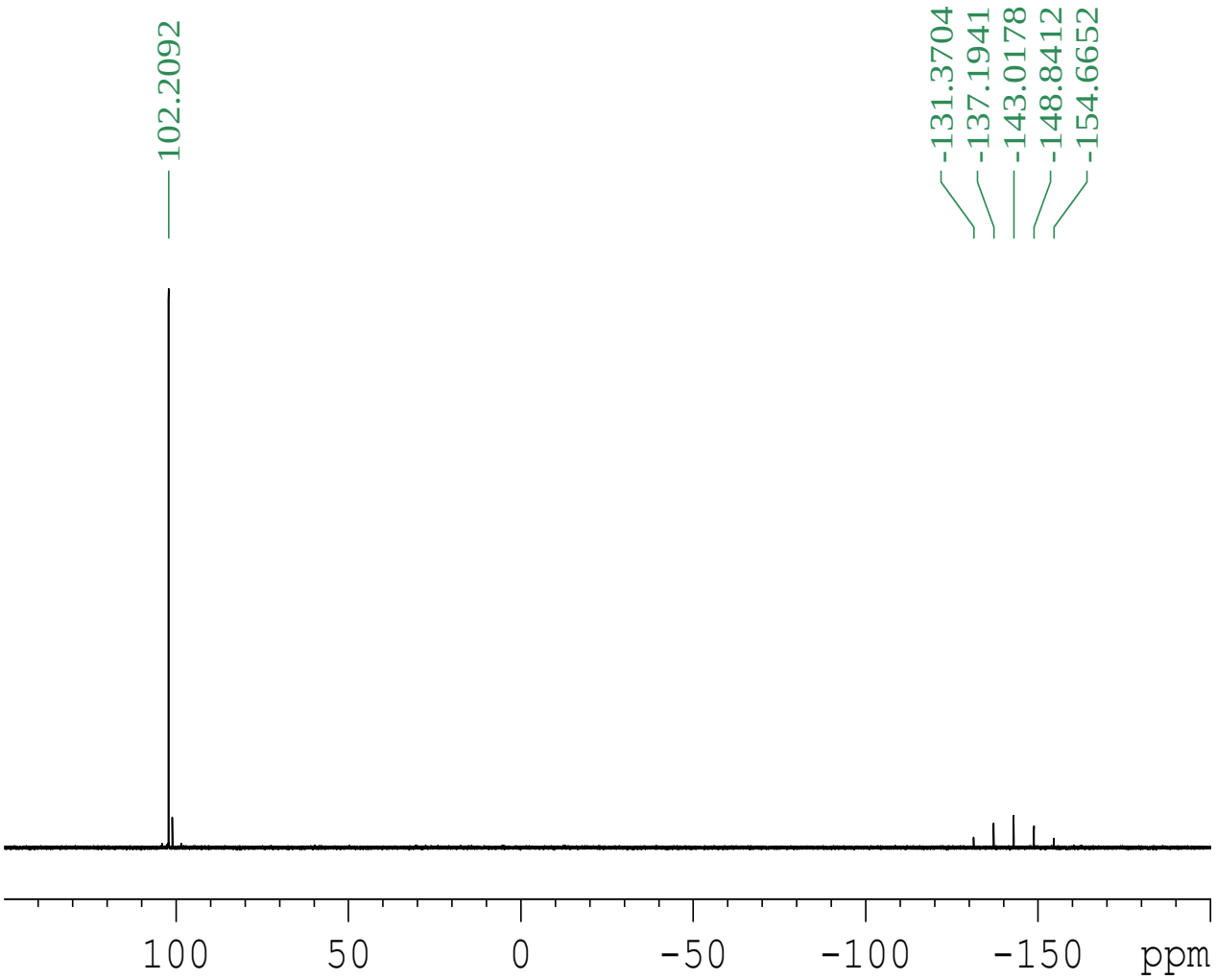

Figure S11. $^{31}P\{^{1}H\}$ NMR spectrum of cluster **1c** in d_6-acetone.

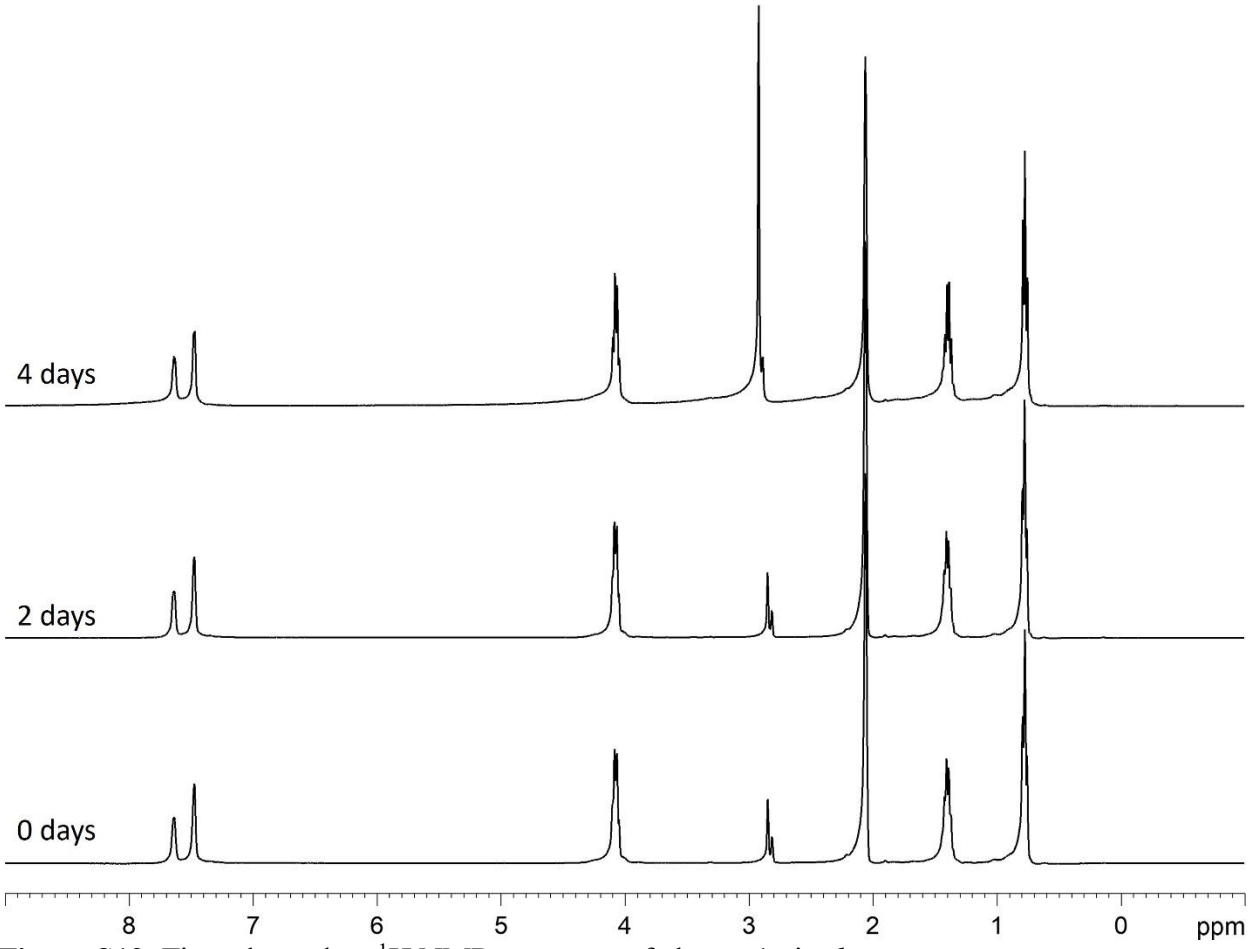

Figure S12. Time-dependent ^{1}H NMR spectrum of cluster **1a** in d_6-acetone.

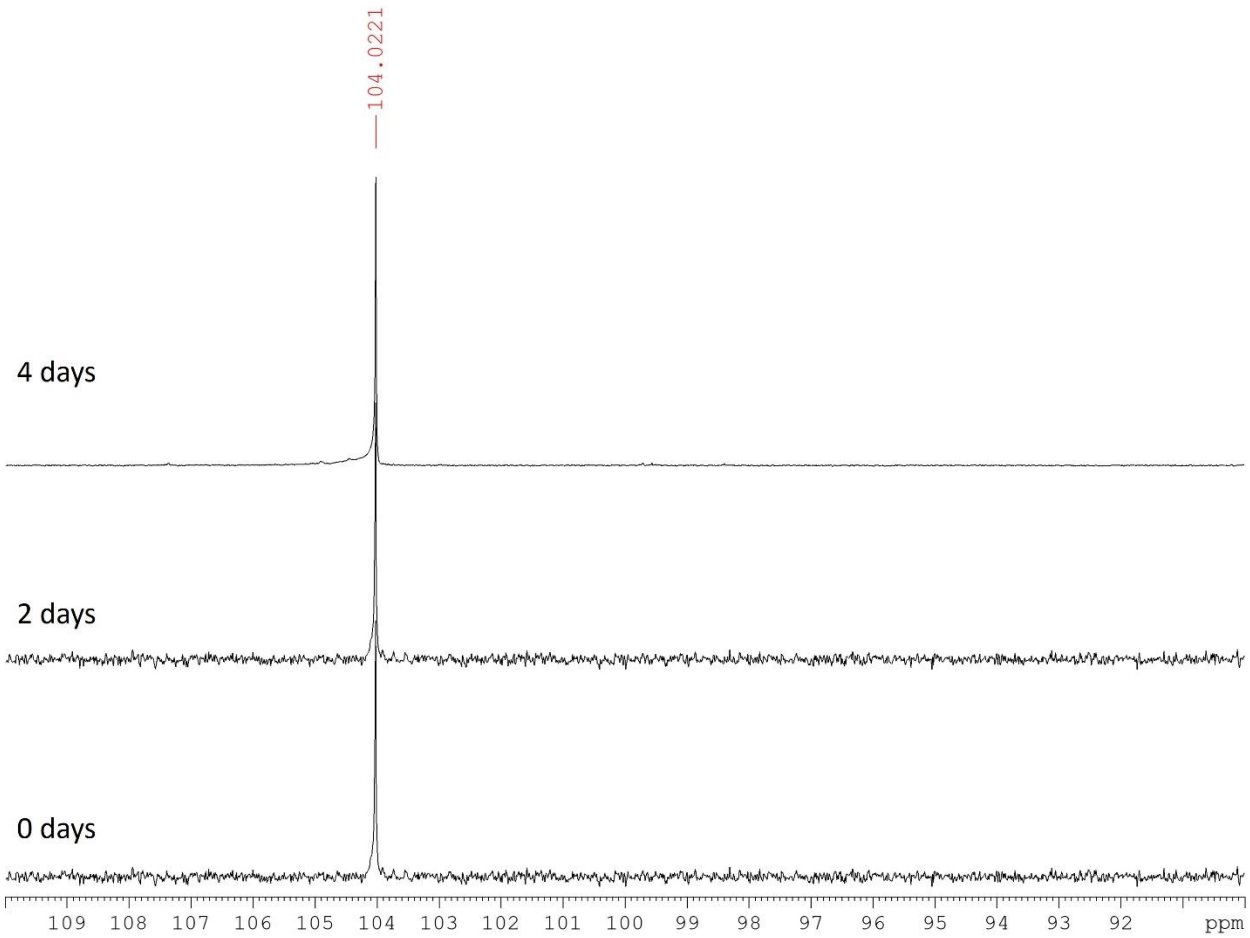

Figure S13. Time-dependent $^{31}P\{^{1}H\}$ NMR spectrum of cluster **1a** in *d6*-acetone.

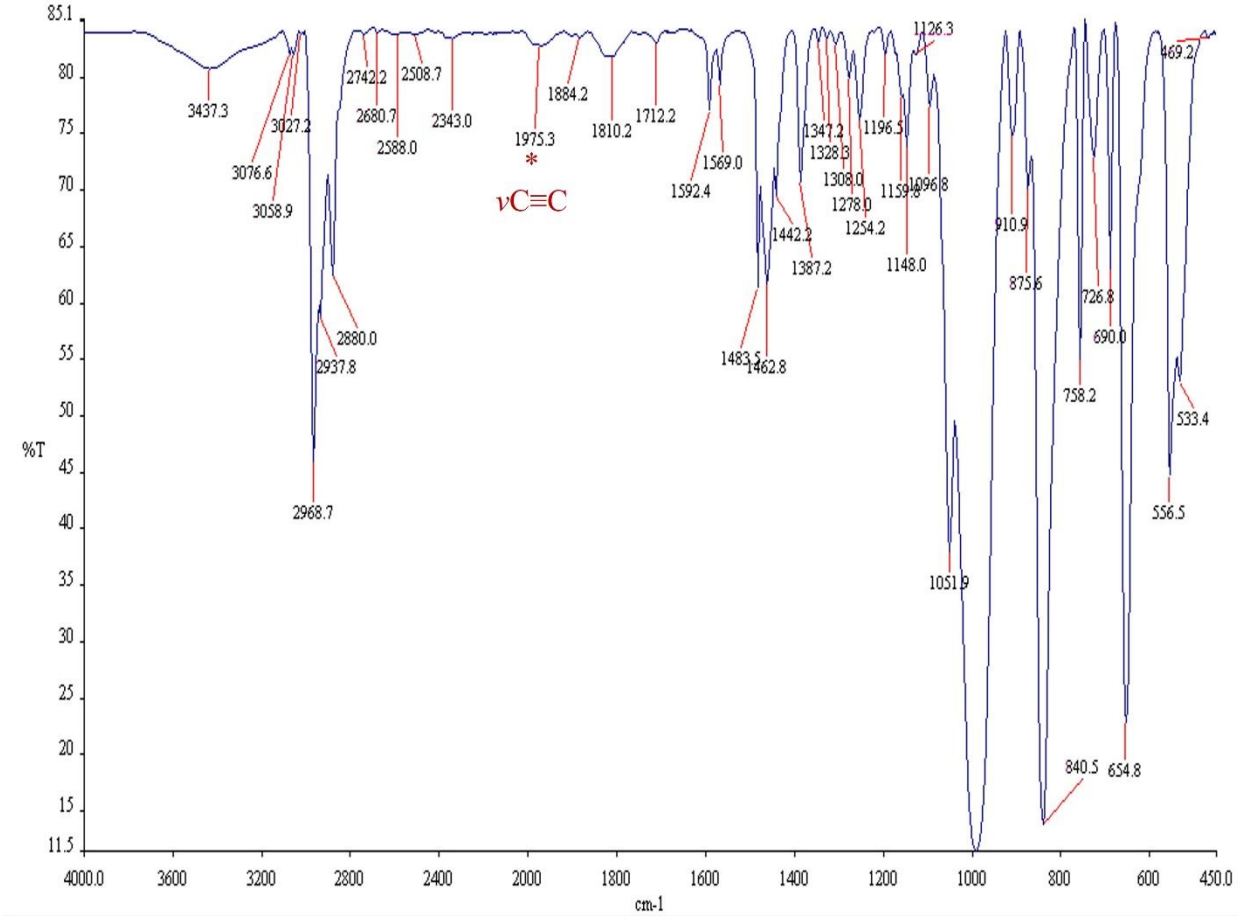

Figure S14. FT-IR spectrum of cluster **1a**.

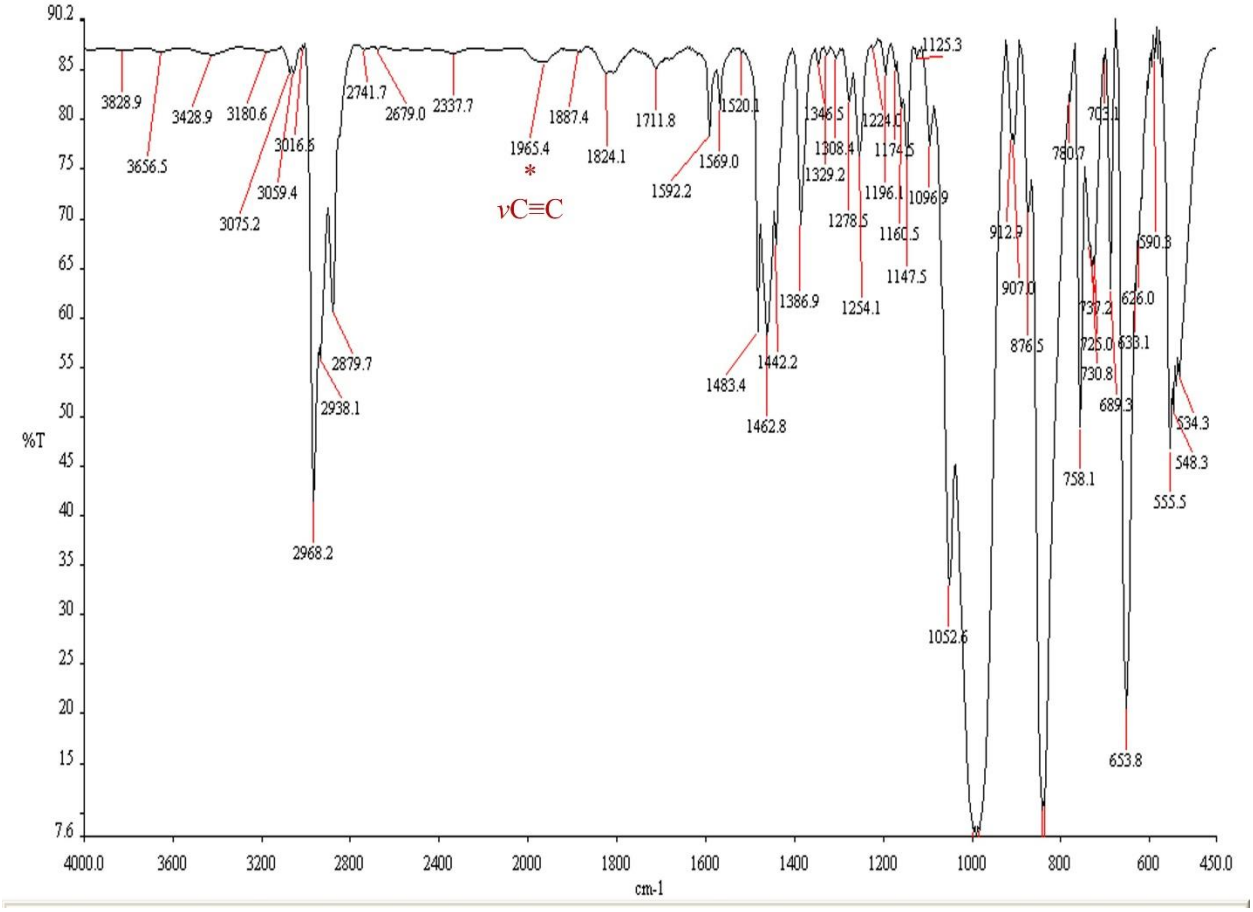

Figure S15. FT-IR spectrum of cluster **1b**.

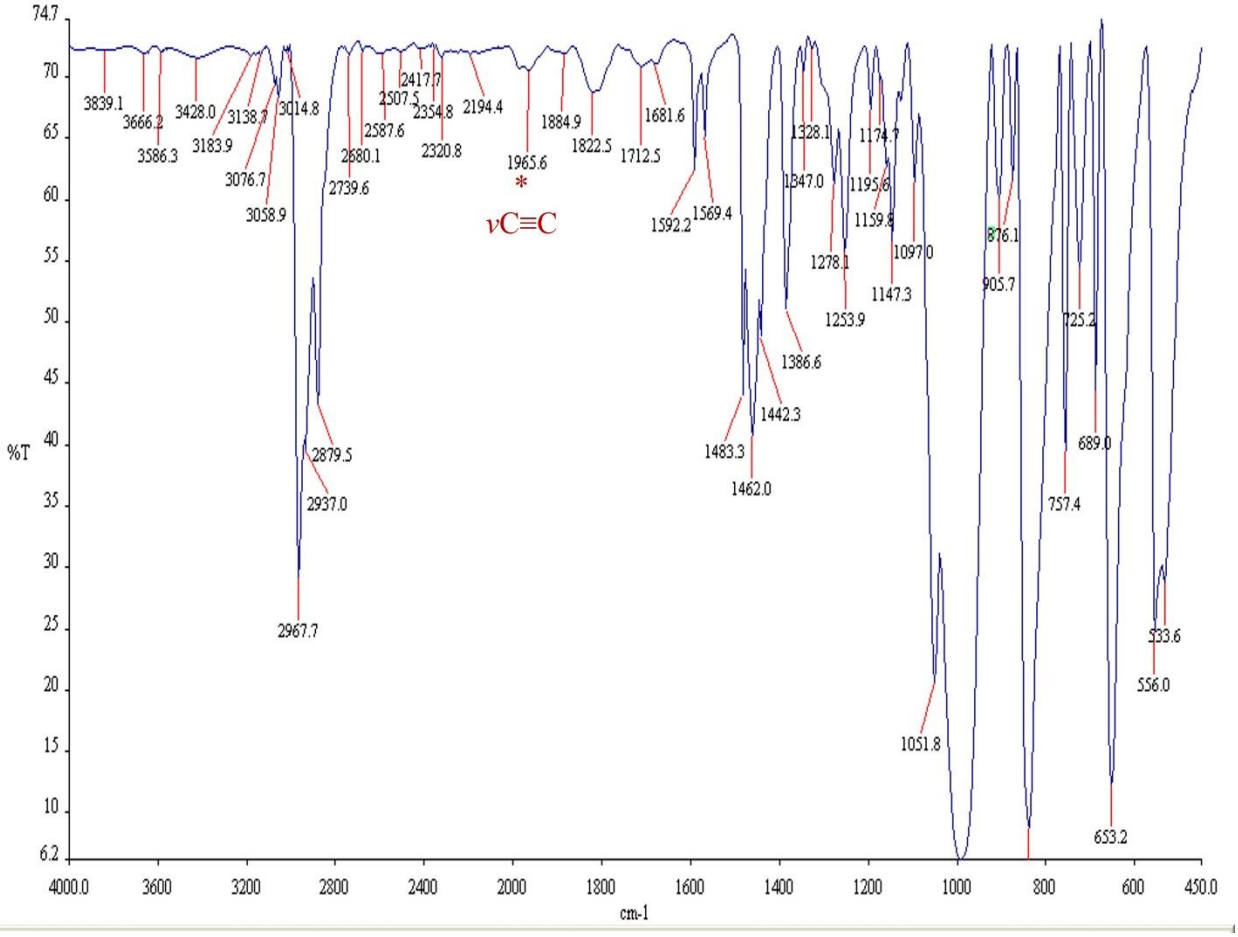

Figure S16. FT-IR spectrum of cluster **1c**.

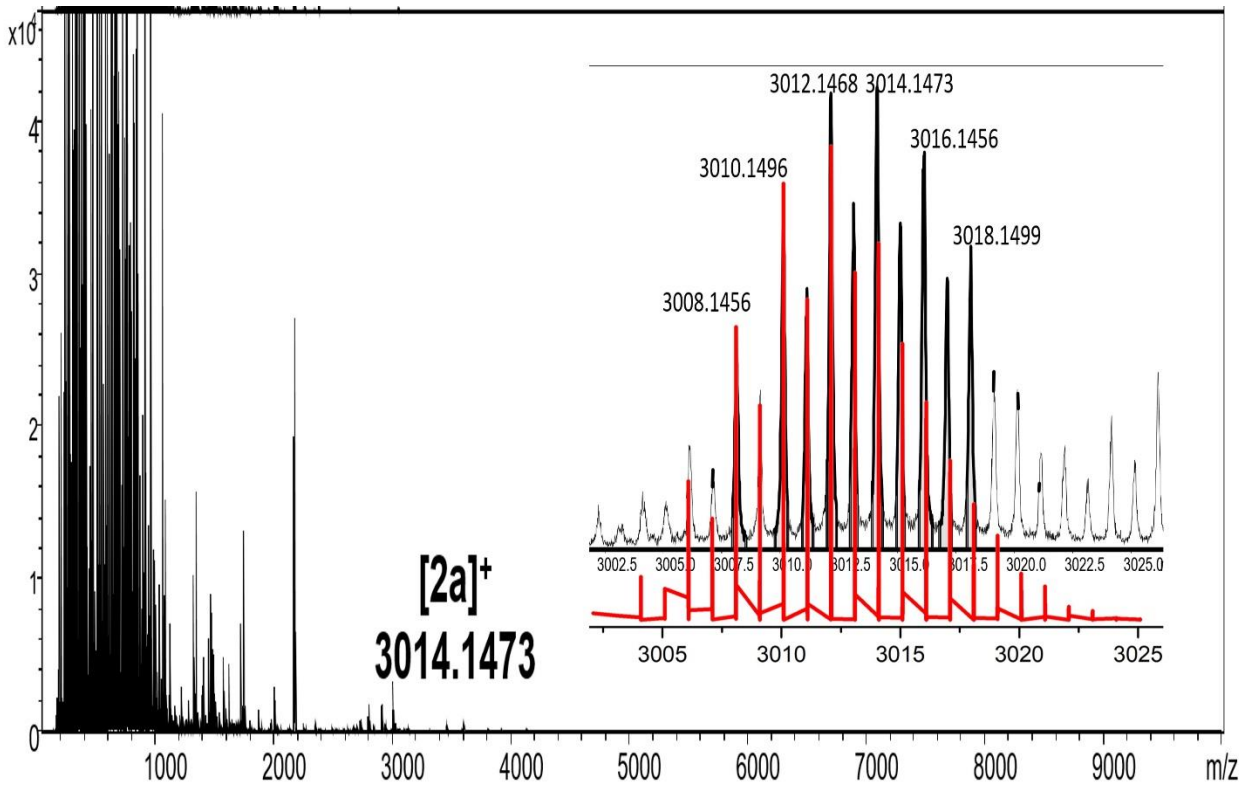

Figure S17. ESI-MS spectra of the cluster [**2a**-PF_6]$^+$ in positive mode. Inset: Experimental in the top (black) and theoretical one in the bottom (red) of [**2a**-PF_6]$^+$.

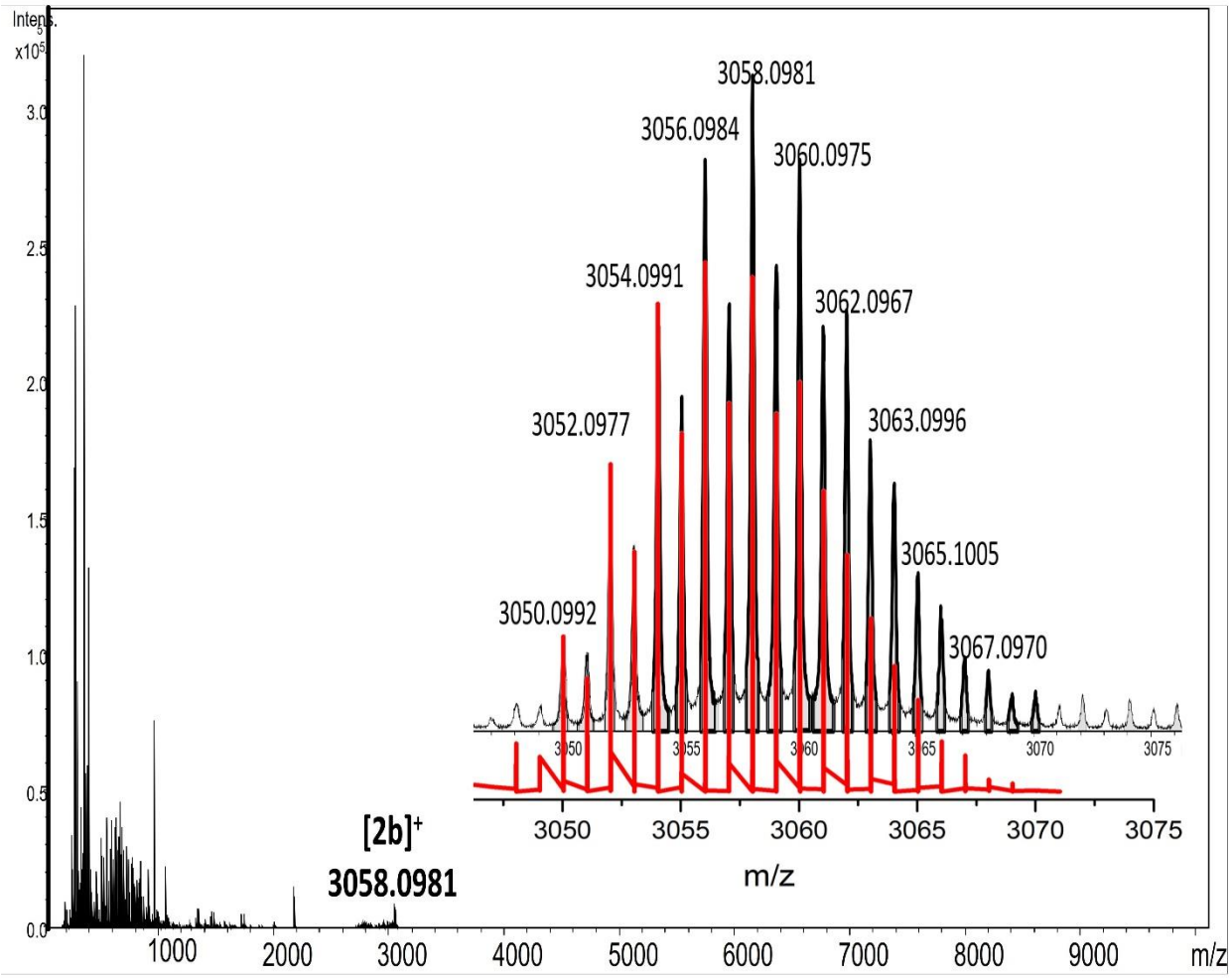

Figure S18. ESI-MS spectra of the cluster [**2b**-PF_6]$^+$ in positive mode. Inset: Experimental in the top (black) and theoretical one in the bottom (red) of [**2b**-PF_6]$^+$.

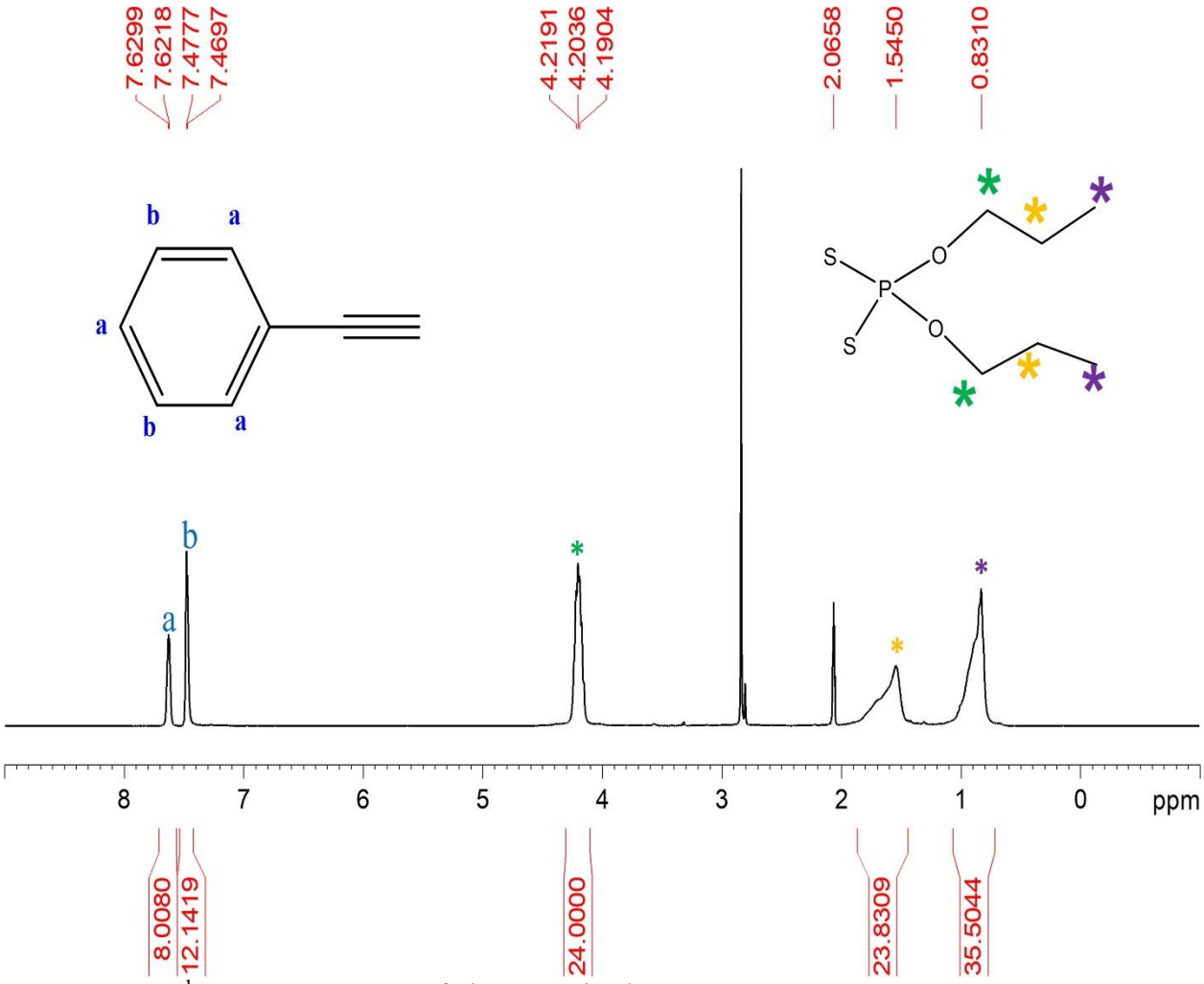

Figure S19. ^{1}H NMR spectrum of cluster **2a** in d_6-acetone.

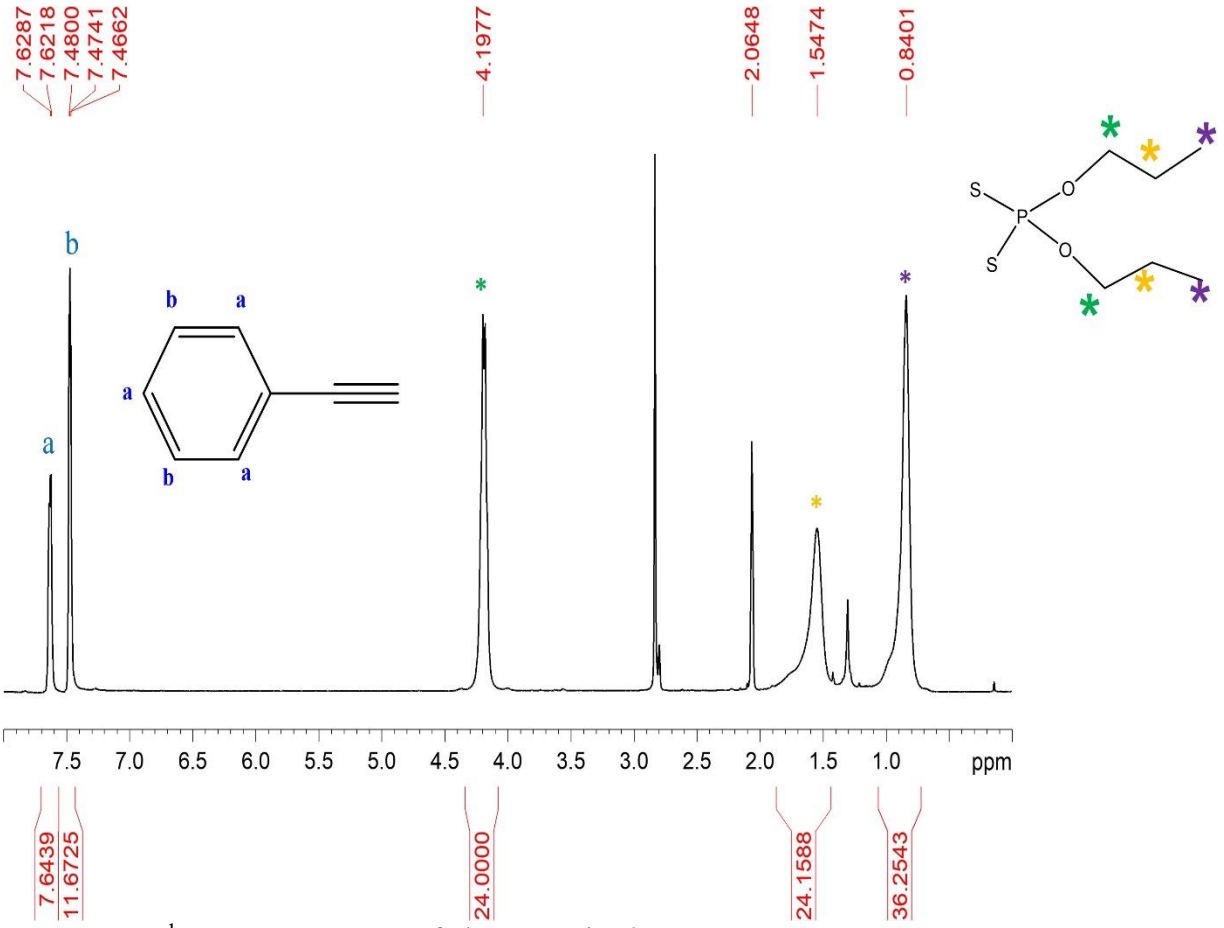

Figure S20. ^{1}H NMR spectrum of cluster **2b** in d_6-acetone.

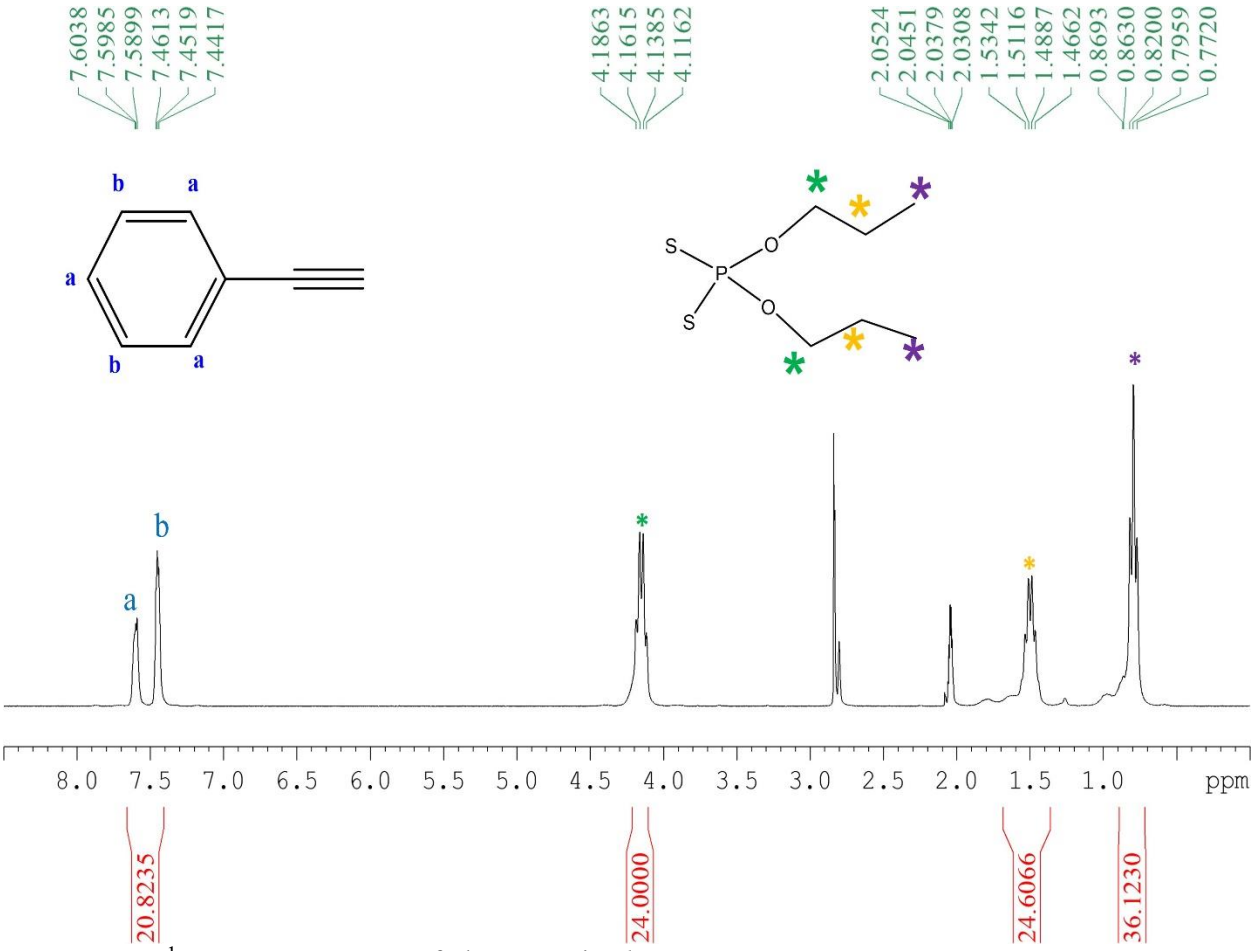

Figure S21. ^{1}H NMR spectrum of cluster **2c** in d_6-acetone.

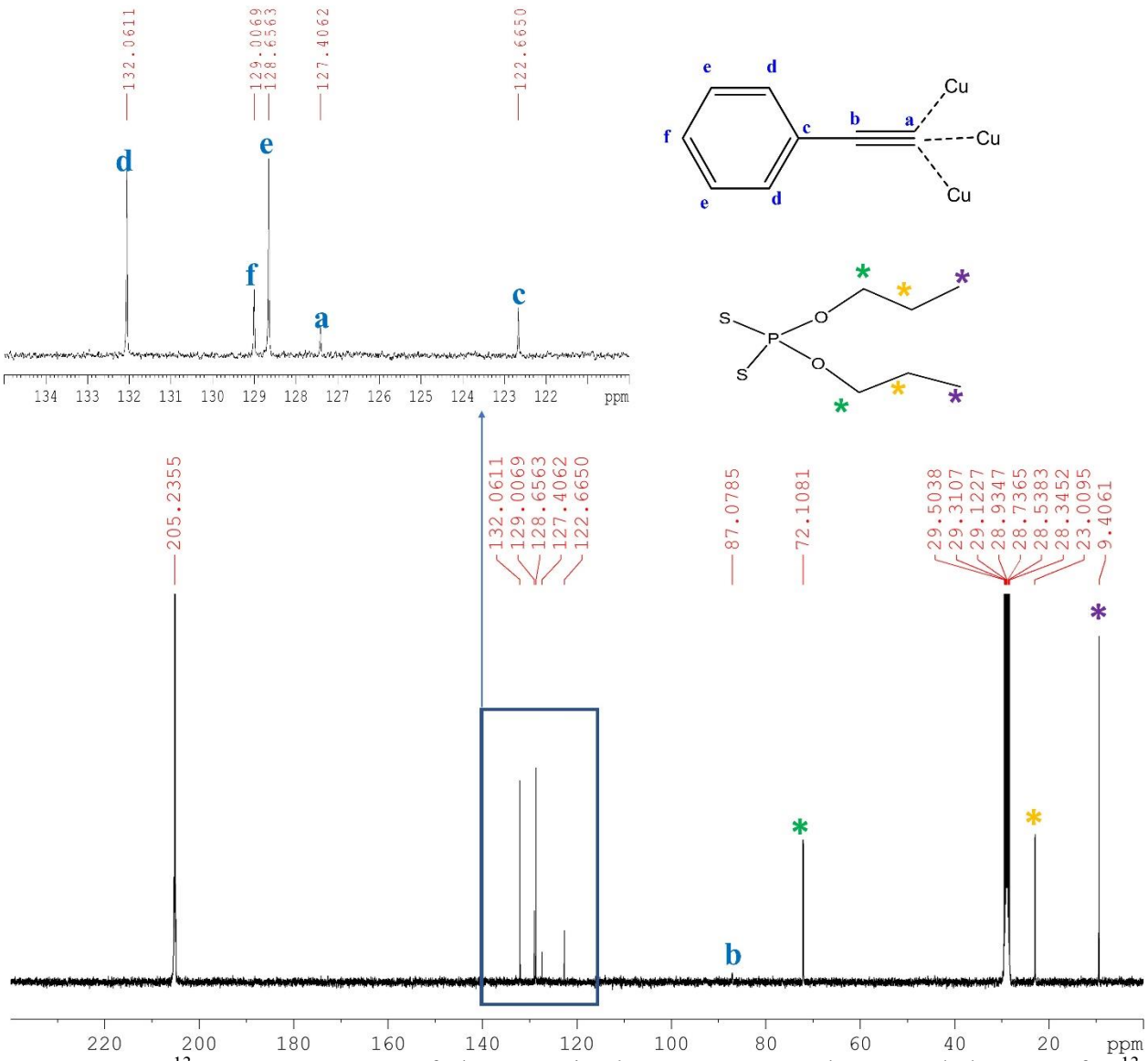

Figure S22. ^{13}C NMR spectrum of cluster **2a** in d_6-acetone. Inset; the expanded spectra for ^{13}C NMR of phenyl rings. The (*, *, and *) highlighted are the ^{13}C NMR of the ^{i}Pr alkyl group in the dithiophosphate ligand.

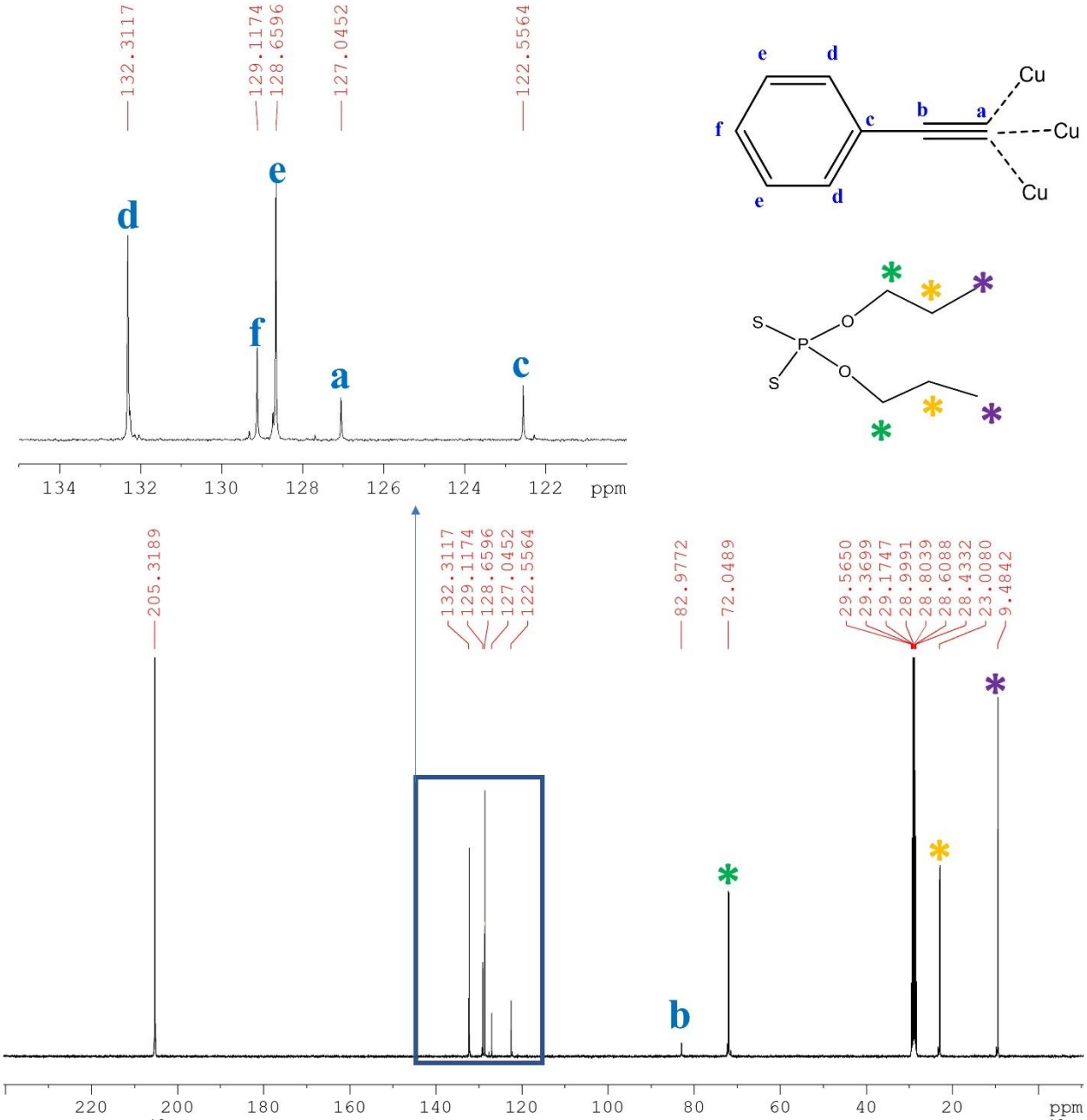

Figure S23. ^{13}C NMR spectrum of cluster **2b** in d_6-acetone. Inset; the expanded spectra for ^{13}C NMR of phenyl rings. The (*, *, and *) highlighted are the ^{13}C NMR of the ^{i}Pr alkyl group in the dithiophosphate ligand.

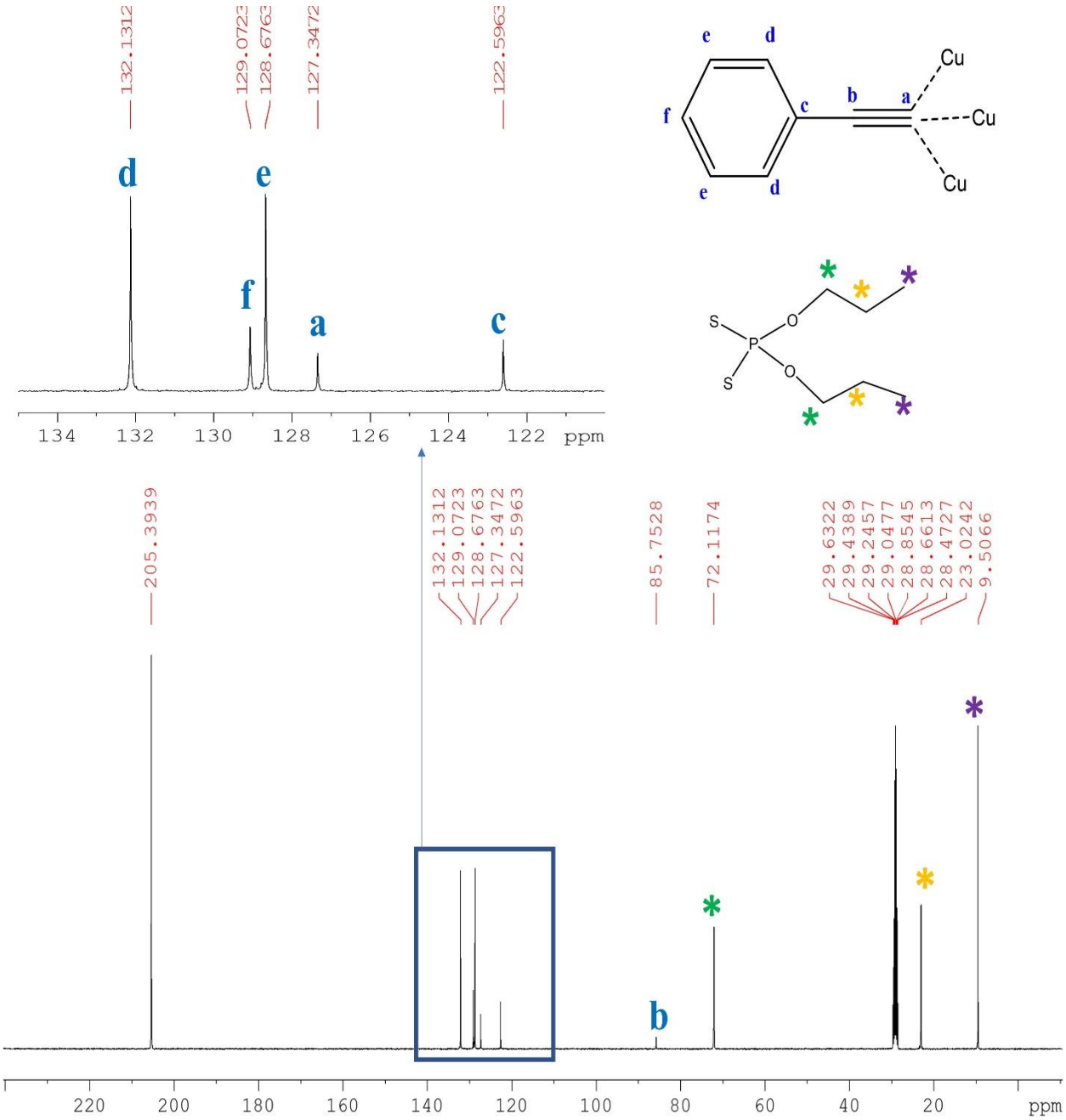

Figure S24. ^{13}C NMR spectrum of cluster **2c** in d_6-acetone. . Inset; the expanded spectra for ^{13}C NMR of phenyl rings. The (*, *, and *) highlighted are the ^{13}C NMR of the ^{i}Pr alkyl group in the dithiophosphate ligand.

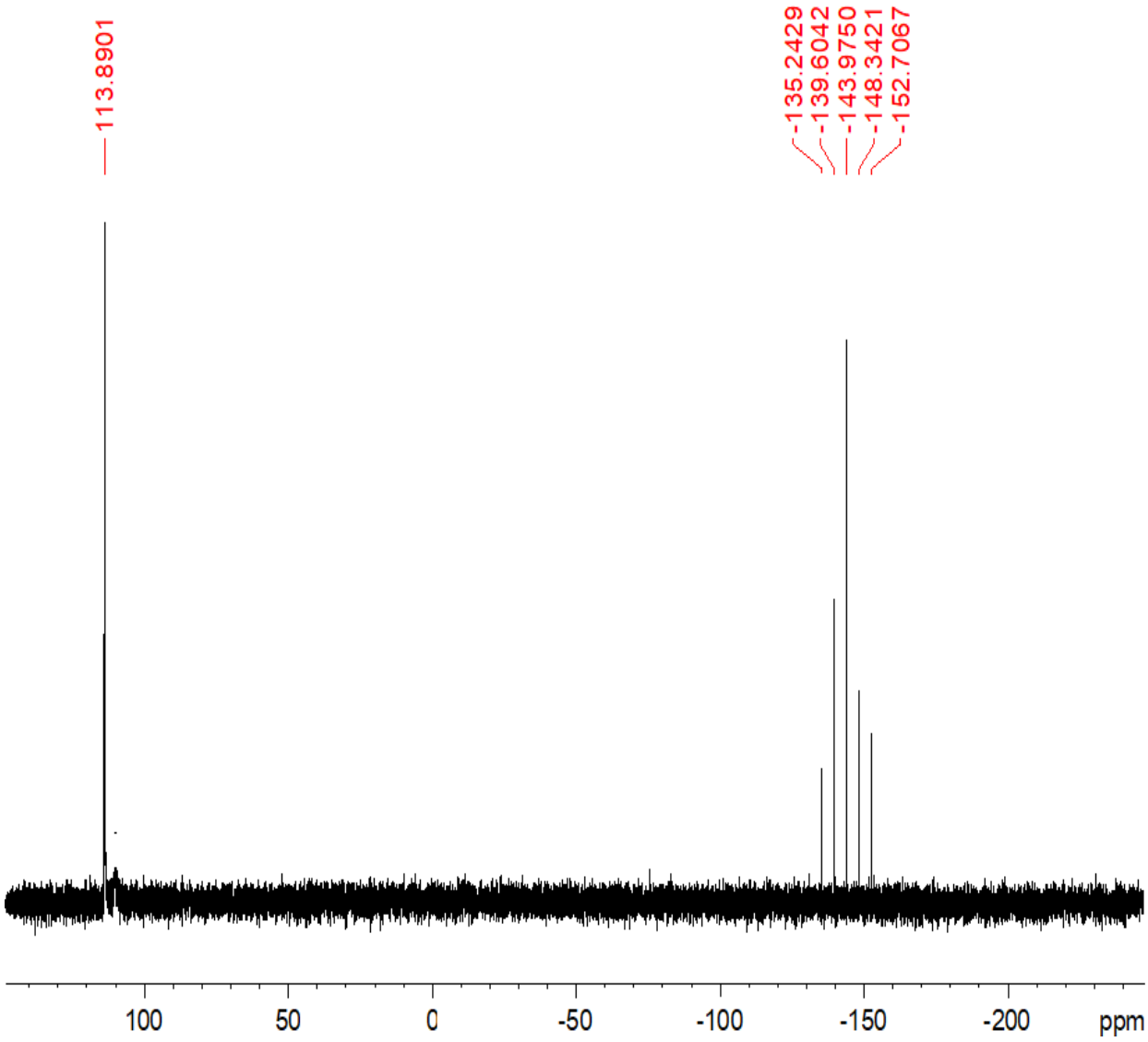

Figure S25. $^{31}P\{^{1}H\}$ NMR spectrum of cluster **2a** in d_6-acetone.

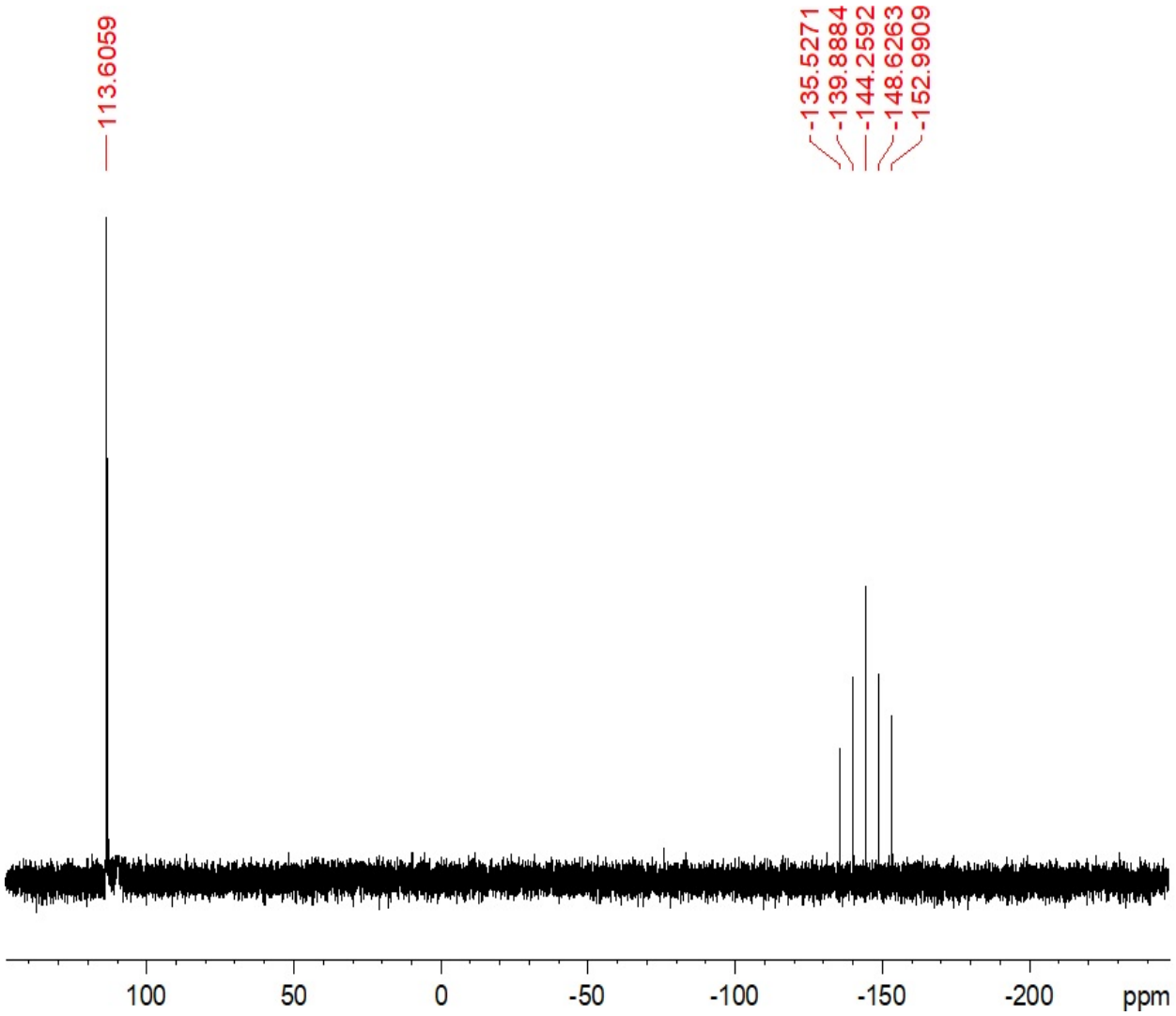

Figure S26. $^{31}P\{^{1}H\}$ NMR spectrum of cluster **2b** in d_6-acetone.

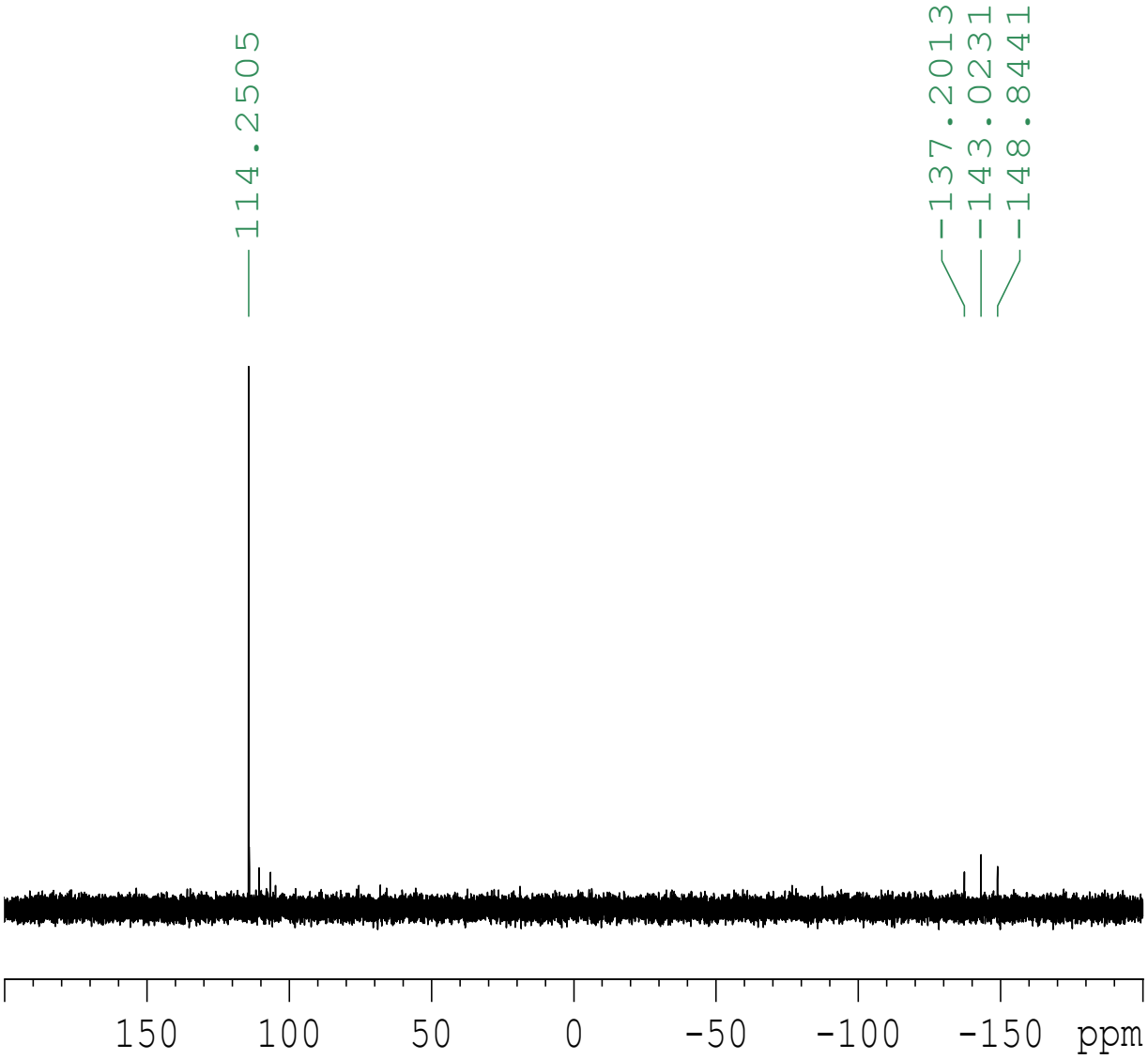

Figure S27. $^{31}P\{^{1}H\}$ NMR spectrum of cluster **2c** in d_6-acetone.

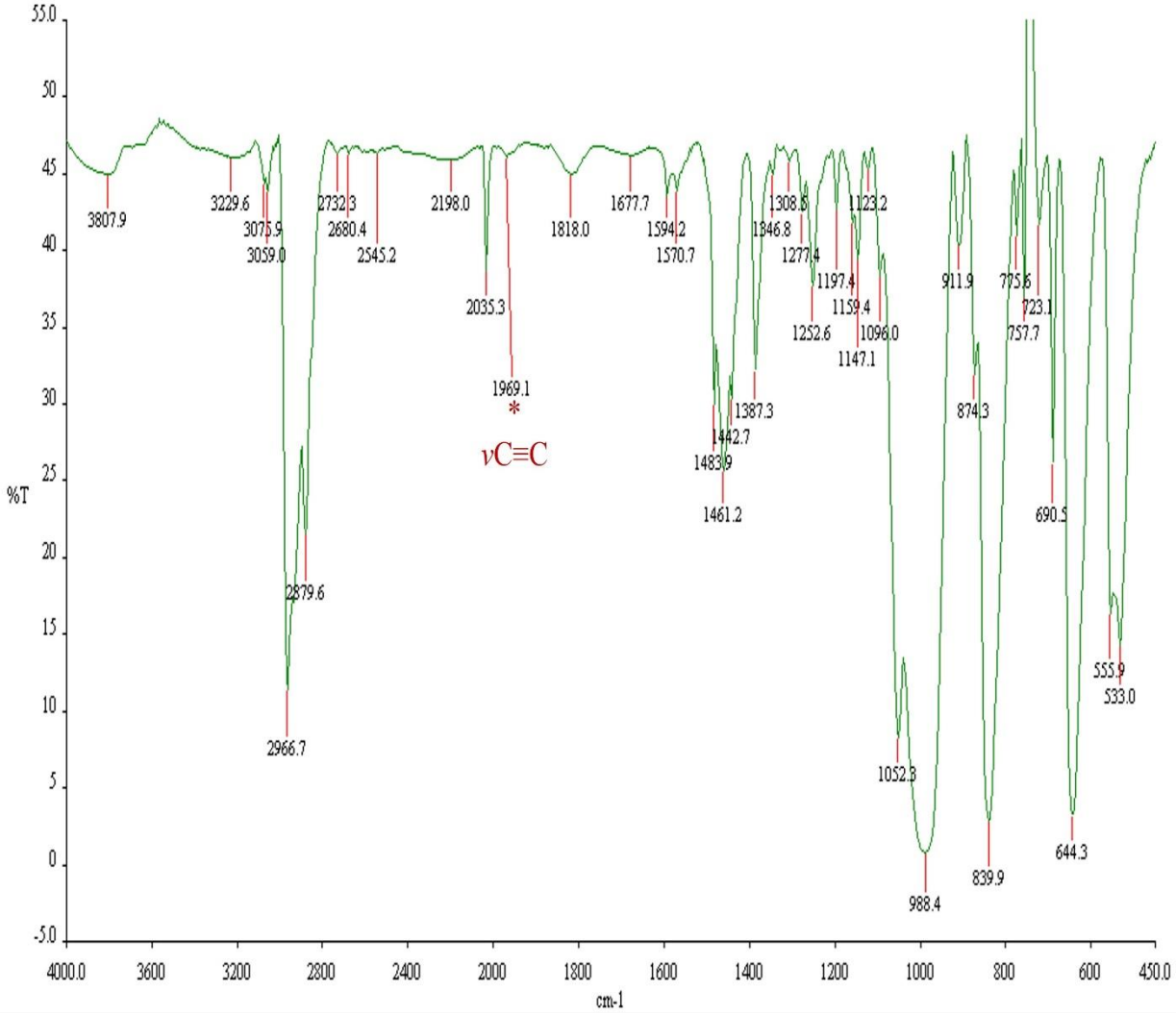

Figure S28. FT-IR spectrum of cluster **2a.**

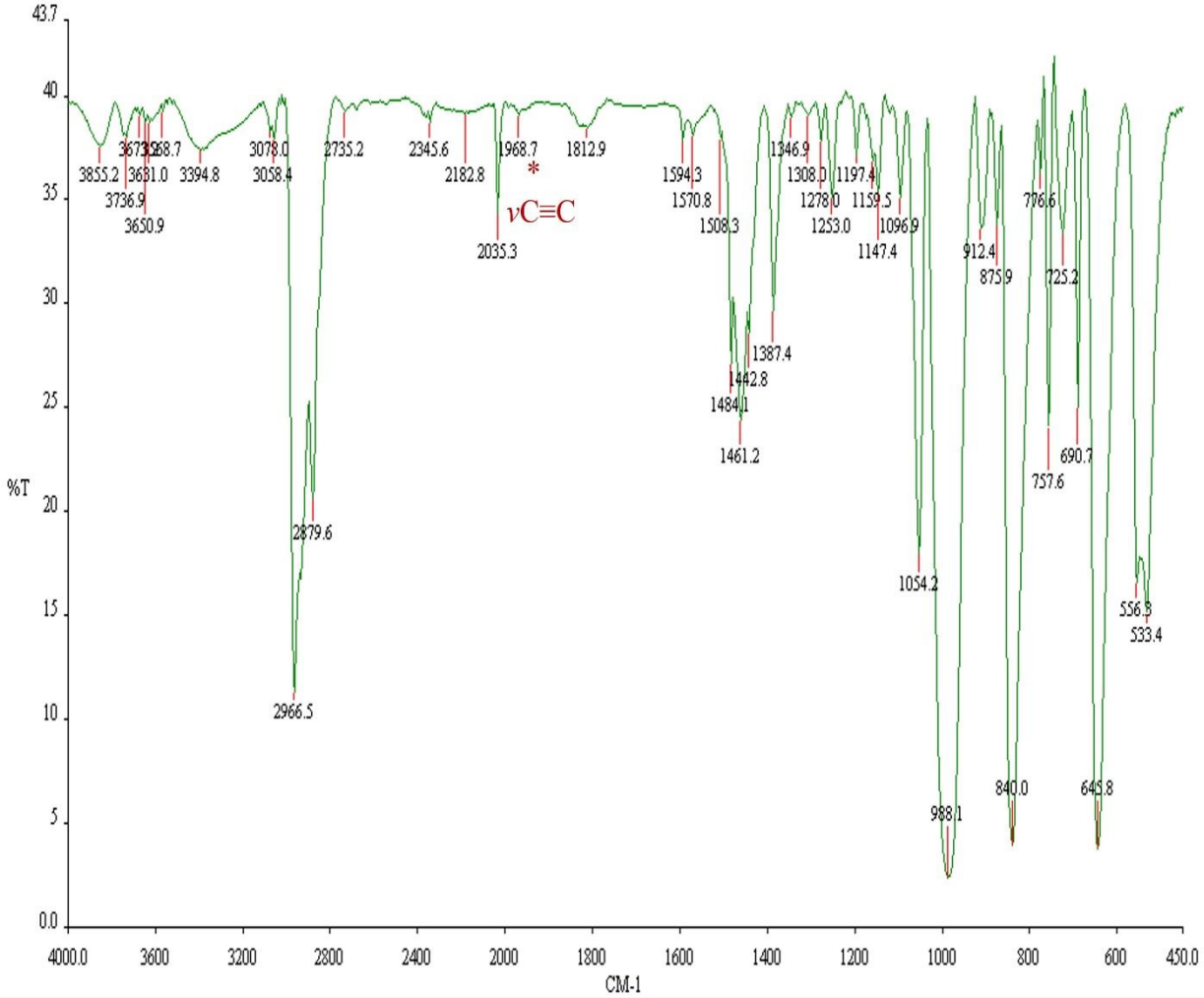

Figure S29. FT-IR spectrum of cluster **2b.**

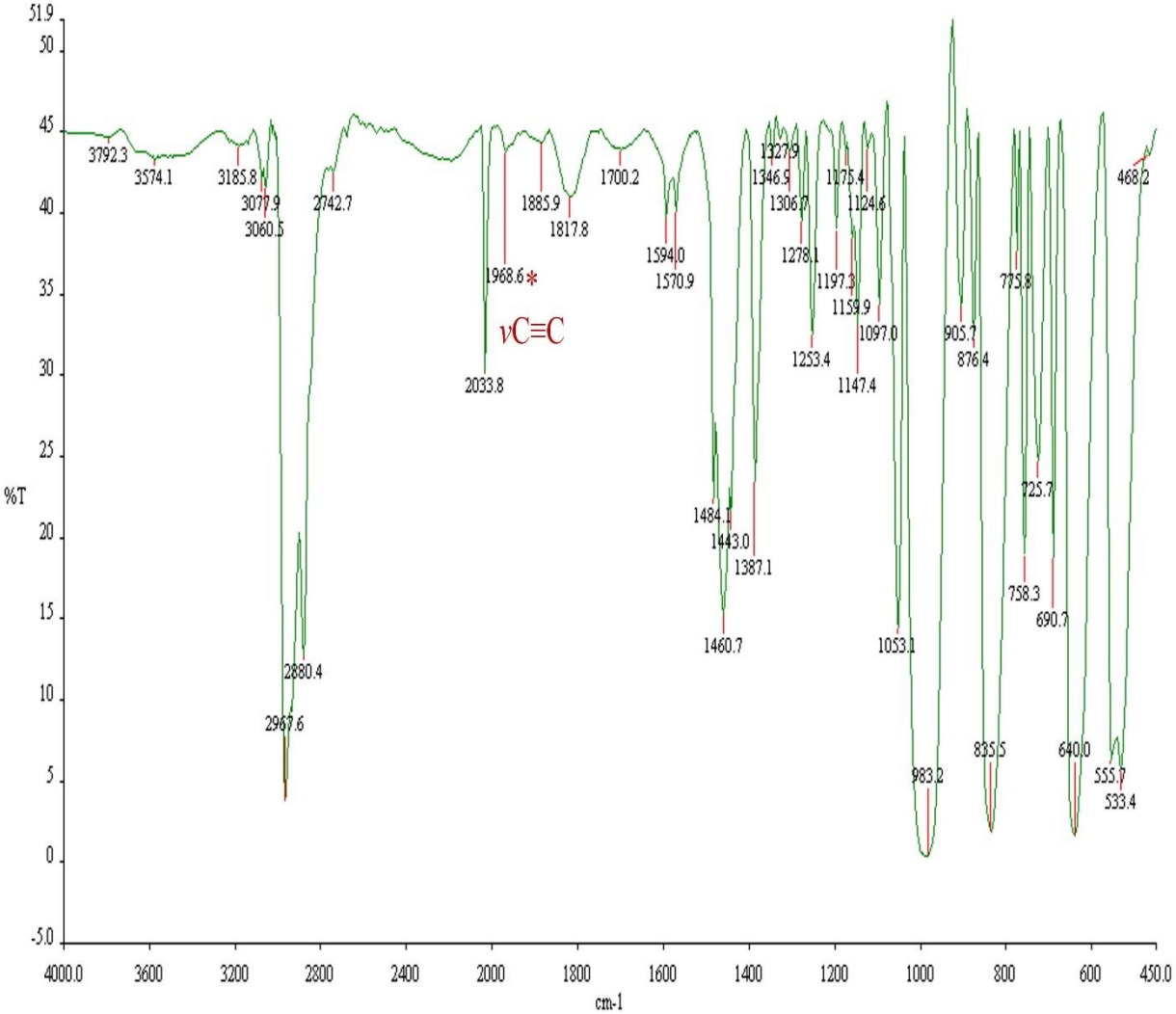

Figure S30. FT-IR spectrum of cluster **2c.**

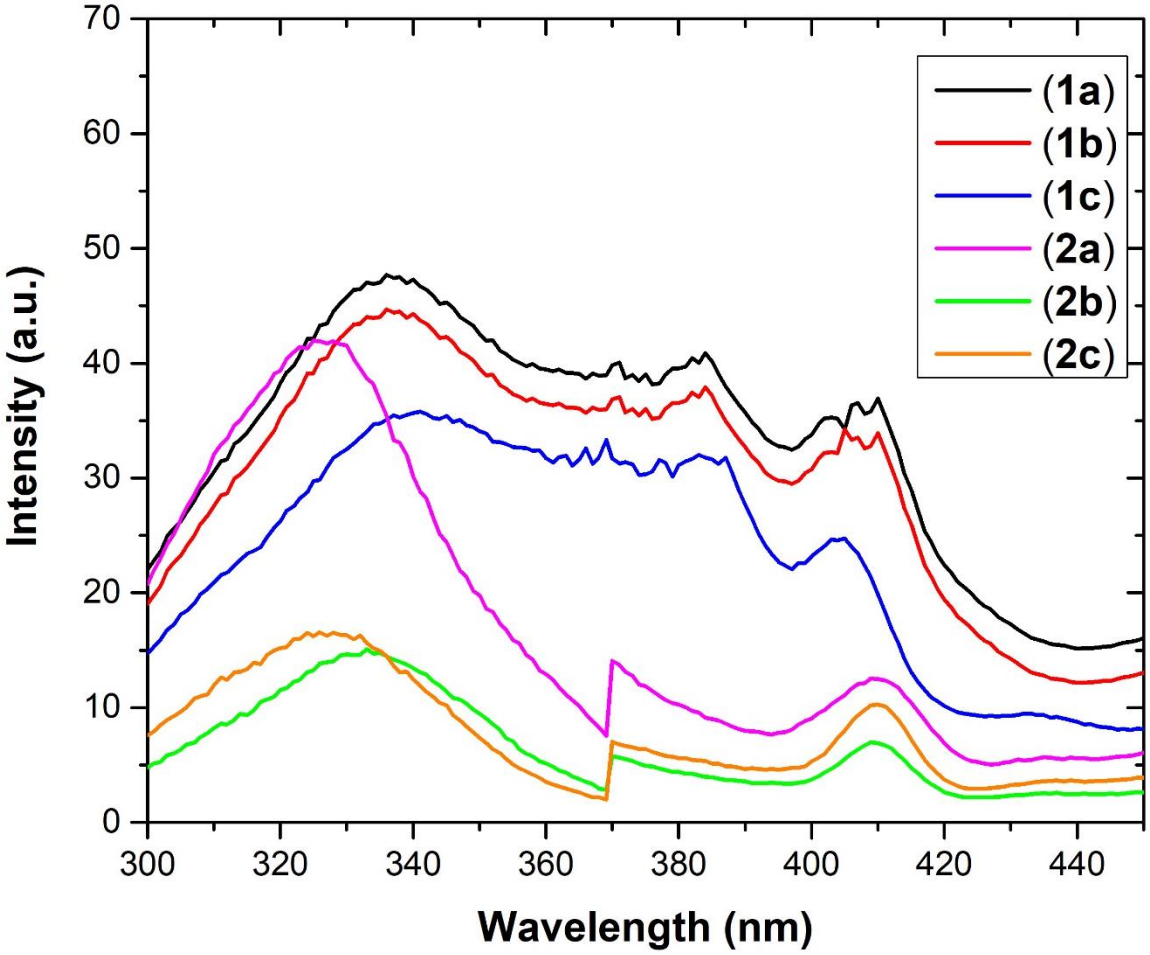

Figure 31. The excitation spectra of cluster **1a-c** and **2a-c** in 2-MeTHF at 77 K.

Table S1. Selected X-ray crystallographic data of **1a-c** and **2a-c**.

	1a	**1b**	**1c**	**2a**	**2b**	**2c**
CCDC number	2169261	2169262	2169263	2169264	2169265	2169266
Empirical formula	$C_{68}H_{104}ClCu_{12}F_6O_{12}P_7S_{12}$	$C_{68}H_{104}BrCu_{12}F_6O_{12}P_7S_{12}$	$C_{68}H_{104}Cu_{12}F_6O_{13}P_7S_{12}\cdot(CH_3)_2CO$	$C_{68}H_{104}Ag_{12}ClF_6O_{12}P_7S_{12}$	$C_{68}H_{104}Ag_{12}BrF_6O_{12}P_7S_{12}$	$C_{68}H_{104}Ag_{12}F_6IO_{12}P_7S_{12}$
Formula weight	2626.95	2671.41	2776.46	3268.99	3203.37	3250.36
Temperature, K	150(2)	150(2)	150(2)	150(2)	150(2)	150(2)
Wavelength, Å	0.71073	0.71073	0.71073	0.71073	0.71073	0.71073
Crystal system	Monoclinic	Monoclinic	Triclinic	Triclinic	Triclinic	Triclinic
Space group	$P2_1/n$	$P2_1/n$	P-1	P-1	P-1	P-1
a, Å	18.626(2)	18.6194(15)	16.7070(19)	21.3242(6)	21.4279(7)	21.4823(3)
b, Å	23.462(3)	23.4762(18)	17.367(2)	22.8389(6)	22.7192(8)	22.6593(9)
c, Å	22.637(3)	22.7144(18)	19.993(2)	23.6053(6)	23.7146(7)	23.8050(9)
α, deg.	90	90	66.877(2)	79.8300(6)	99.8543(7)	99.8379(8)
β, deg.	90.394(3)	90.280(2)	83.253(2)	89.9697(6)	90.3872(7)	90.4695(9)
γ, deg.	90	90	71.002(2)	63.8667(6)	116.2836(7)	116.3596(8)
Volume, $Å^3$	9892.1(19)	9928.6(14)	5044.1(10)	10120.0(5)	10153.9(6)	10183.7(7)
Z	4	4	2	4	4	4
Calculated density, Mg m^{-3}	1.764	1.787	1.828	2.080	2.095	2.120
Absorption coefficient, mm^{-1}	2.978	3.342	3.202	2.712	3.070	2.971
Crystal size, mm^3	0.30x0.17x0.10	0.10x0.07x0.05	0.20x0.12x0.04	0.25x0.24x0.07	0.25x0.16x0.05	0.25x0.13x0.10
θ_{max}, deg.	27.143	25.000	24.999	27.154	24.999	25.000
Reflections collected / unique	123710/21882 [R_{int}= 0.0372]	58959/17453 [R_{int}=0.0367]	32764/17534 [R_{int}= 0.0242]	80345/43760 [R_{int}= 0.0171]	60899/35292 [R_{int}= 0.0196]	75557/35369 [R_{int}= 0.0208]
Completeness, %	100	99.9	98.6	98.6	98.7	98.6
restraints / parameters	469/1079	523/1111	134/1171	922/2212	1053/2237	929/2219
GOF	1.038	1.015	1.026	1.022	1.017	1.047
[a] $R1$, [b] $wR2$ [I>2σ(I)]	$R1$ = 0.0302, $wR2$ = 0.0704	$R1$= 0.0310, $wR2$= 0.0680	$R1$=0.0612, $wR2$= 0.1743	$R1$= 0.0325, $wR2$= 0.0762	$R1$= 0.0350, $wR2$= 0.0931	$R1$= 0.0415, $wR2$= 0.1023
[a] $R1$, [b] $wR2$ (all data)	$R1$ = 0.0366, $wR2$ = 0.0740	$R1$= 0.0460, $wR2$= 0.0750	$R1$=0.0784, $wR2$= 0.1933	$R1$= 0.0404, $wR2$= 0.0816	$R2$= 0.0438, $wR2$= 0.1002	$R1$= 0.0496, $wR2$= 0.1103
Largest diff. peak / hole, e $Å^{-3}$	1.228/-1.460	1.043/-0.796	2.710/-0.872	2.131/-1.783	1.924/-1.529	2.389/-2.226

[a] $R1 = \Sigma \mid \mid F_o \mid - \mid Fc \mid \mid / \Sigma \mid F_o \mid$. [b] $wR2 = \{\Sigma[w(F_o^2 - F_c^2)^2]/\Sigma[w(F_o^2)^2]\}^{1/2}$